European Journal of Medicinal Chemistry 128 (2017) 274–286

Contents lists available at ScienceDirect

European Journal of Medicinal Chemistry

journal homepage: http://www.elsevier.com/locate/ejmech

Research paper

Rational design of reversible inhibitors for trehalose 6-phosphate phosphatases

Chunliang Liu, Debra Dunaway-Mariano*, Patrick S. Mariano**

Department of Chemistry and Chemical Biology, University of New Mexico, Albuquerque, NM 87131, USA

ARTICLE INFO

Article history:
Received 3 January 2017
Received in revised form
1 February 2017
Accepted 3 February 2017
Available online 4 February 2017

Keywords:
HAD phosphatase
Trehalose 6-sulfate
Trehalose 6-phosphate phosphatase
T6PP inhibitor
Antihelminthic

ABSTRACT

In some organisms, environmental stress triggers trehalose biosynthesis that is catalyzed collectively by trehalose 6-phosphate synthase, and trehalose 6-phosphate phosphatase (T6PP). T6PP catalyzes the hydrolysis of trehalose 6-phosphate (T6P) to trehalose and inorganic phosphate and is a promising target for the development of antibacterial, antifungal and antihelminthic therapeutics. Herein, we report the design, synthesis and evaluation of a library of aryl D-glucopyranoside 6-sulfates to serve as prototypes for small molecule T6PP inhibitors. Steady-state kinetic techniques were used to measure inhibition constants (K_i) of a panel of structurally diverse T6PP orthologs derived from the pathogens *Brugia malayi*, *Ascaris suum*, *Mycobacterium tuberculosis*, *Shigella boydii* and *Salmonella typhimurium*. The binding affinities of the most active inhibitor of these T6PP orthologs, 4-*n*-octylphenyl α-D-glucopyranoside 6-sulfate (**9a**), were found to be in the low micromolar range. The K_i of **9a** with the *B. malayi* T6PP ortholog is 5.3 ± 0.6 μM, 70-fold smaller than the substrate Michaelis constant. The binding specificity of **9a** was demonstrated using several representative sugar phosphate phosphatases from the HAD enzyme superfamily, the T6PP protein fold family of origin. Lastly, correlations drawn between T6PP active site structure, inhibitor structure and inhibitor binding affinity suggest that the aryl D-glucopyranoside 6-sulfate prototypes will find future applications as a platform for development of tailored second-generation T6PP inhibitors.

1. Introduction

The (α-1,α′-1)-glucose dimer trehalose is produced by specialized bacteria, fungi, plants and nematodes in response to environmental stress [1–6]. Trehalose biosynthesis is catalyzed, collectively, by trehalose 6-phosphate synthase (T6PS), which catalyzes the condensation of glucose 6-phosphate and uridine 5′-diphosphoglucose (UDP-glucose) to trehalose 6-phosphate (T6P), and trehalose 6-phosphate phosphatase (T6PP), which catalyzes the hydrolysis of T6P to trehalose and inorganic phosphate (see Fig. 1) [7,8]. Gene silencing experiments, carried out with *Mycobacterium tuberculosis*, *Cryptococcus neoformans* and *C. gattii*, *Aspergillus fumigatus*, *Candida albicans*, *Caenorhabditis elegans* and *Brugia malayi*, demonstrated the sensitivity of microbial and nematodal human pathogens to the disruption of the trehalose pathway [9–16]. T6PP, the subject of our work, is required both for trehalose production and for the prevention of T6P accumulation and associated toxicity [11,15]. Despite the considerable discussion given to T6PP as a platform for the development of antibacterial, antifungal and antihelminthic therapeutics [9,11,12,15,16], T6PP inhibitors have not yet been reported. In this article, we report the synthesis and evaluation of a library of first generation T6PP inhibitors designed using a modular approach.

2. Results and discussion

2.1. Inhibitor design

The T6PP inhibitor design was guided by the X-ray crystal structure of the T6PP ortholog from the archaeon *Thermoplasma acidophilum* (Ta-T6PP) [17]. The Ta-T6PP backbone fold conforms to that of the type C2 Haloalkanoic Acid Dehalogenase (HAD)

* Corresponding author. Department of Chemistry and Chemical Biology, University of New Mexico, MSC03 2060, 300 Terrace St. NE, Albuquerque, NM 87131-0001, USA.
** Corresponding author. Department of Chemistry and Chemical Biology, University of New Mexico, MSC03 2060, 300 Terrace St. NE, Albuquerque, NM 87131-0001, USA.
E-mail addresses: dd39@unm.edu (D. Dunaway-Mariano), mariano@unm.edu (P.S. Mariano).

http://dx.doi.org/10.1016/j.ejmech.2017.02.001
0223-5234/

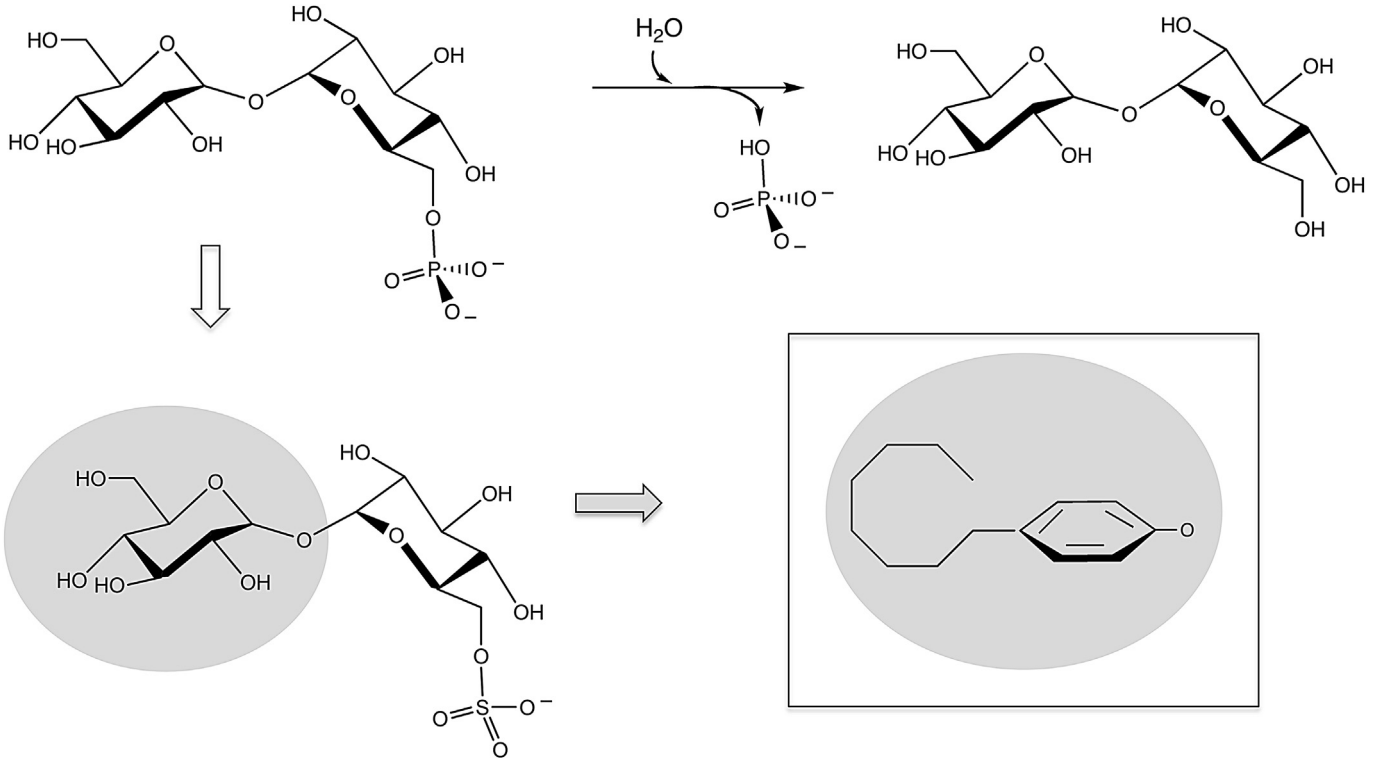

Fig. 1. An illustration of the trehalose 6-phosphate phosphatase-catalyzed hydrolysis of trehalose 6-phosphate to trehalose and inorganic phosphate and the sequential modifications made to the substrate structure in forming the first generation inhibitor 4-*n*-octylphenyl α-D-glucopyranoside-6-sulfate.

superfamily phosphatase [18]. As with other phosphatases of this structural class, T6PP is comprised of a Rossmann-fold catalytic domain and the inserted α/β-fold cap domain. Ensuing structure determinations, first on the T6PP ortholog from the pathogenic nematode *B. malayi* (Bm-T6PP) [19], and most recently on the T6PP orthologs from fungal pathogens *C. albicans*, *C. neoformans* and *A. fumigatus* [20] and the bacterial pathogen *M. tuberculosis* [21], have illuminated the structural determinants of substrate recognition.

A comparative analysis of the T6PP X-ray structures identifies the active site formed at the cap domain-catalytic domain interface and provides insight into the domain dynamics associated with catalytic cycling. To illustrate, the superposition of the structures of the T6P complex of the T6PP-D24 N (site-directed mutant) from *C. neoformans* (colored cyan) and the (unbound) *apo*-TPP from *A. fumigatus* (green) is shown in Fig. 2A. From the outset, we had assumed that T6PP, like other HAD phosphatases possessing a mobile cap domain, would undergo changes in domain-domain association as required to open the catalytic site for substrate binding, close it for catalysis, and open it for product release. Indeed, the structures of the fungal T6PP orthologs define two cap domain-catalytic domain orientations, one in which the active site is open to enable ligand exchange (hereafter referred to as the "open conformer") and the other in which the active site is closed for catalysis (the "closed conformer").

Although the suggested T6PP substrate induced-fit mechanism (depicted by the cartoon in Fig. 2B) confers substrate specificity, it also subtracts from the intrinsic binding energy, hence binding affinity [22]. Furthermore, the carbohydrate portion of the substrate is an unlikely source of binding energy because its partitioning between solvent and the T6PP binding site relies primarily on the entropic advantage gained from intramolecular multi-site binding created by the active site [23]. Weak T6P binding is consistent with the large steady-state K_m values (200–1600 μM) observed for T6PP orthologs [19–21,24–28], and confirmed by using substrate-fragment analysis [28]. The analysis showed that phosphate, glucose 6-phosphate and trehalose do not generate sufficient binding energy to overcome the entropy penalty intrinsic to protein-ligand association. Thus, stable complexes are not formed [28].

With this information in hand and the original apo-TaT6PP structure to guide inhibitor design, we pursued the divide-and-conquer strategy depicted in Fig. 1. The plan was to retailor the substrate by first replacing the labile phosphate group with a stable mimetic, and then substitute the carbohydrate portion with a structural module tailored to complement the substrate binding site. Because the T6P phosphate group binds to a polar pocket, where it favorably interacts with the Mg^{2+} cofactor and several stringently conserved electropositive amino acid residues (Fig. 2B), we limited our search to tetrahedral oxyanions. This led to the ultimate discovery that the sulfate group is best suited for this purpose [28]. Trehalose 6-sulfate (T6S) thus became the platform for tailoring the trehalose unit for enhanced binding affinity.

Inspection of the T6PP structure given in Fig. 2A, reveals that the two substrate glucosyl units are bound in starkly different environments. Whereas the hydroxyl groups of inner glucosyl moiety (the one that is phosphorylated) collectively form multiple hydrogen bonds with the charged side chains of a cap domain Glu-Lys-Glu triad, the outer glucosyl unit (the one that is not phosphorylated) is bound through interactions with the main chain amide groups of an encompassing loop from the catalytic domain. For the purpose of inhibitor design, the inner glucosyl unit was left intact and used for tethering a structural motif designed to extract binding energy through optimized interaction with the active site. Because the "cap-closing" interactions between the T6P inner glucosyl hydroxyl groups are retained, the T6PP inhibitor will

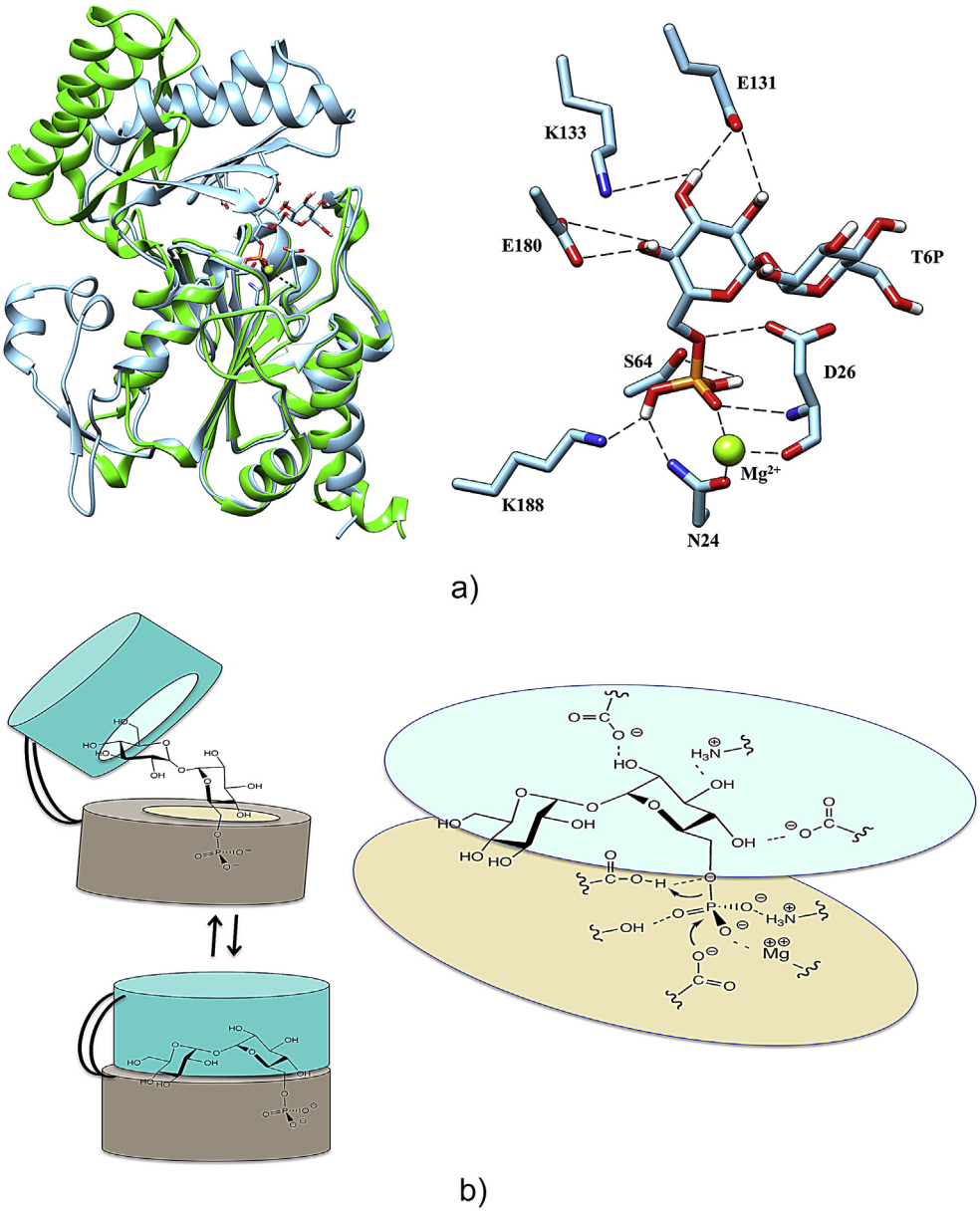

Fig. 2. (**A**). Left: Superposition of the structures of the T6P complex of the D24 N mutant T6PP from *C. neoformans* (cyan, PDB: 5DX9) and the *apo*-T6PP from *A. fumigatus* (green, PDB:5DXL). Right: View of the bound T6P ligand and the binding interacts that occur with the phosphate group and with the Glu-Lys-Glu triad of the cap domain. (**B**). Cartoon depiction of the trehalose 6-phosphate phosphatase mechanism of substrate binding by induced cap domain-catalytic domain association stabilized by the noncovalent bonding interactions with the bridging substrate T6P. (For interpretation of the references to colour in this figure legend, the reader is referred to the web version of this article.)

complement the space-restricted, desolvated-binding site of the closed conformer. Given that we were initially unaware of the key role played by the inner-glucosyl unit in cap domain binding, the choice to use it in the template was fortuitous.

In the design of T6PP inhibitors, we selected an aryl group to replace the outer glucosyl unit in view of the fact that it carries both binding site compatibility and synthetic versatility. Specifically, as a protein ligand, the π-electron cloud of the aromatic ring engages in electrostatic binding interactions with nearby polar residues [29], and its departure from solvent gives rise to the desired "hydrophobic effect" [30] associated with tight ligand binding. Just as important, the aromatic ring also serves as an ideal scaffold to introduce strategically placed substituents. In the sections that follow, we describe the synthesis and evaluation of the library of aryl D-glucopyranoside 6-sulfate derivatives created using this simple modular design.

2.2. Inhibitor library synthesis and evaluation

The library of aryl D-glucopyranoside 6-sulfate derivatives (and related structures), and the strategies and protocols used in their synthesis are given in Fig. 3 and the Experimental section. The results from testing the derivatives for T6PP inhibition are given in Tables 1 and 2.

Our objective in preparing and evaluating the synthetic library was to identify a tight binding inhibitor and to correlate the binding affinity with specific features of the inhibitor structure. To begin, we selected the phenyl derivatives to test the aryl D-glucopyranoside 6-sulfate platform with the T6PP ortholog in hand, Bm-T6PP. The selection of Bm-T6PP to serve in the initial exploratory study

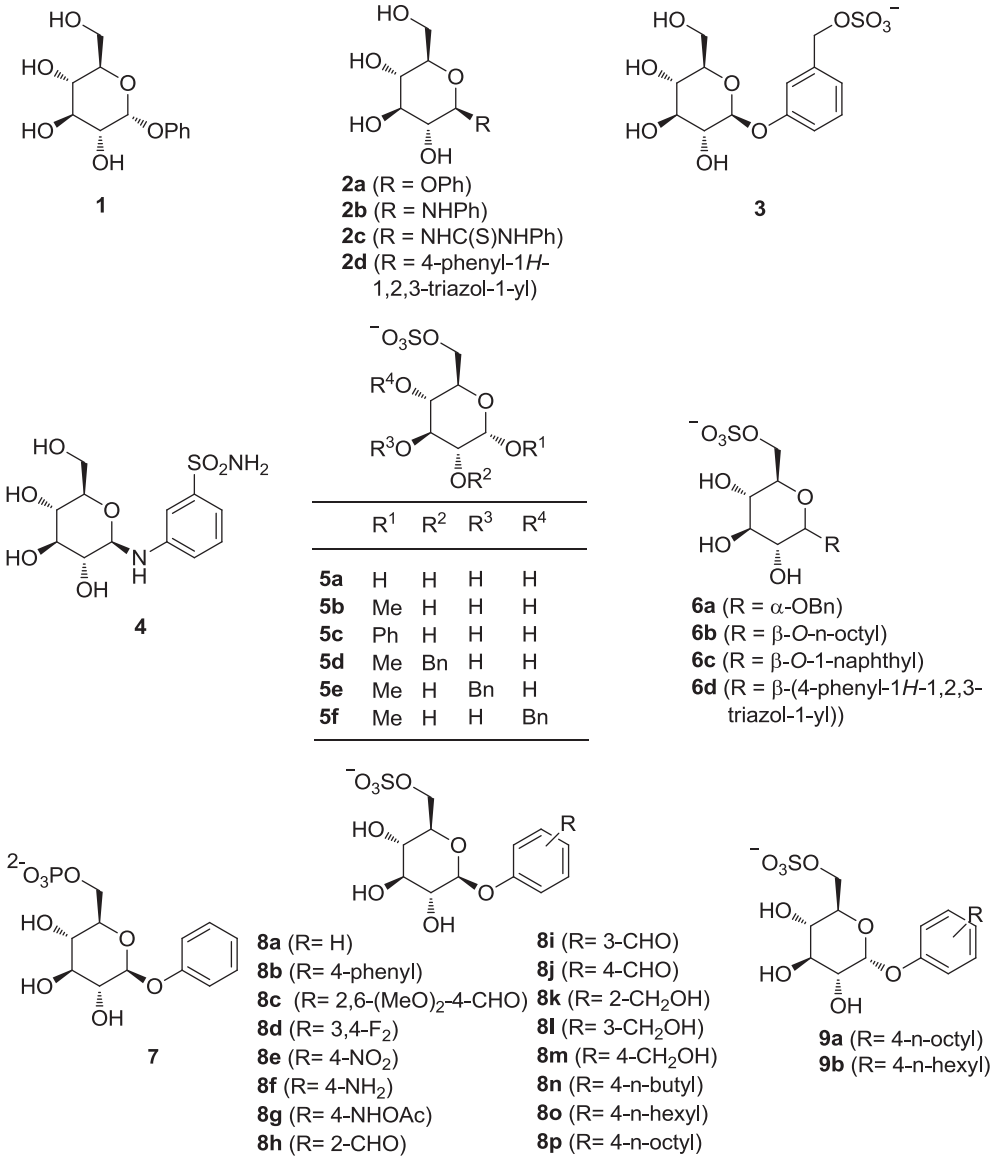

Fig. 3. The library of compounds synthesized for testing as inhibitors of T6PP.

Table 1
Steady-state inhibition constants determined at pH 7.5 and 25 °C for the targeted inhibitors of T6PP-catalyzed hydrolysis of trehalose 6-phosphate (T6P). See Fig. 3 to find the chemicals structures of the inhibitors and the Experimental section for details.

Inhibitor	Bm-T6PP K_i (μM)	As-T6PP K_i (μM)	Sb-T6PP K_i (μM)	St-T6PP K_i (μM)	Mt-T6PP K_i (μM)
9a	5.3 ± 0.6	80 ± 10	21 ± 3	56 ± 6	~100
9b	80 ± 10	350 ± 30	78 ± 9	280 ± 30	>400
8p	60 ± 10	180 ± 20	13 ± 2	120 ± 20	>300
8o	~200	~200	140 ± 20	>400	>400
T6P K_m (μM)	360 ± 60[a]	230 ± 70[b]	690 ± 70[b]	310 ± 40[b]	500 ± 100[b]

[a] Reported in Farelli et al. [19].
[b] Reported in Liu et al. [28].

was also fortuitous because it turned out to be the most highly inhibited among the five T6PP orthologs probed.

The phenyl α- (**5c**) and β- (**8a**) D-glucopyranoside 6-sulfate anomers prepared and tested for inhibition of T6P hydrolysis catalyzed by Bm-T6PP, proved to be reversible competitive inhibitors with K_i = 320 ± 30 μM and 800 ± 100 μM, respectively. We imagined that the phenyl D-glucopyranoside 6-sulfate ligand would bind to the active site oriented in a manner analogous to that of bound substrate, with the glucosyl 6-sulfate substituting for the glucosyl 6-phosphate and the phenyl ring substituting for the outer glucosyl unit. To check this assumption, we prepared phenyl β-D-glucopyranoside 6-phosphate (**7**) and tested its substrate activity by measuring the rate of T6PP-catalyzed phosphate release. Whereas the glucose 6-phosphate itself shows no substrate activity (<0.0001 s^{-1}) [28], the corresponding *O*-phenyl derivative undergoes catalyzed hydrolysis at the rate ca. 0.01 s^{-1} (Table S1, Supplementary Information). This activity, although no greater than 1% that of T6P hydrolysis, suggests that **7** binds, albeit weakly, to the active site in a "T6P-like" orientation. Furthermore, one might speculate that the phenyl D-glucopyranoside 6-phosphate α-anomer, compared to the (accessible) β-anomer tested, would likely display more activity because the T6P C1 configuration is α.

To enhance the binding affinity of the corresponding phenyl D-glucopyranoside 6-sulfate inhibitor, a nonpolar group was added to the phenyl ring. The anticipated desolvation of this group into a

Table 2
V_I/V values (fraction of enzyme that is not bound with the inhibitor) measured at pH 7.5 and 25 °C for the library of inhibitors shown in Fig. 3. The initial velocity V of T6PP-catalyzed hydrolysis of T6P at half saturation ([T6PP] = K_m) is compared to the initial velocity (V_I) measured in the presence of 1 mM inhibitor. See the Experimental section for details.

V_I/V					
Compound	Bm-T6PP	Mt-T6PP	Sb-T6PP	As-T6PP	St-T6PP
T6S	0.13	0.43	0.22	0.21	0.01
Trehalose	0.98	0.83	1.01	0.97	0.88
1	0.96	0.88	0.86	0.97	1
2a	1.12	0.81	0.9	1	0.87
2b	1	0.88	0.92	0.97	0.77
2c	0.99	1.04	0.92	0.81	1.09
2d	0.85	0.95	1	0.96	0.9
3	0.59	0.96	0.8	0.98	0.85
4	1.05	1.17	0.85	0.96	1
5a	0.93	0.97	0.75	0.94	0.84
5b	0.8	0.91	1	1.07	1.04
5c	0.42	1.17	0.76	0.71	0.64
5d	0.53	1.01	1	0.96	0.95
5e	0.67	1.16	0.84	1.04	0.99
5f	0.68	1.11	0.95	0.99	0.97
6a	0.07	0.83	0.74	0.86	0.47
6b	0.72	0.83	0.79	0.9	0.54
6c	0.85	0.85	0.85	0.91	0.8
6d	0.98	0.98	0.9	0.76	0.97
7	0.79	0.94	0.94	0.98	0.77
8a	0.52	0.94	0.76	0.92	0.81
8b	0.58	0.58	0.84	0.9	0.85
8c	0.55	1.09	1	0.94	0.96
8d	0.74	0.8	0.92	0.88	0.89
8e	0.64	1.27	0.77	0.83	0.68
8f	0.63	1	1.03	0.74	0.94
8g	0.87	0.94	0.88	0.9	0.85
8h	0.79	1.17	0.96	0.99	0.85
8i	1.05	0.67	0.81	0.78	0.95
8j	1	0.87	1.06	0.81	0.87
8k	0.89	0.89	0.85	0.9	0.73
8l	0.69	0.69	0.46	0.63	0.77
8m	0.68	0.85	0.67	0.76	0.79
8p	0.07	0.42	0.04	0.02	0.01

suitable sub-compartment of the active site, should in principle, augment inhibitor binding via the "hydrophobic effect". n-Hexyl and n-octyl substituents were selected because each provides a sufficient number of methylene units for desolvation. In addition, the conformational flexibility of the long aliphatic chain facilitates binding to a compatible surface in the active site. The K_i values determined for the α- and β-anomers of the *p*-hexylphenyl substrates, **9b** and **8o**, and those of the *p*-octylphenyl substrates, **9a** and **8p**, are given in Table 1. A comparison of K_i values reveals that the aliphatic group enhances binding, that the octyl group is superior to the hexyl group, and that inhibitors having the α-configuration at their anomeric centers display the tightest binding. The K_i of **9a**, determined with the *B. malayi* T6PP ortholog to be 5.3 ± 0.6 μM, is 70-fold smaller than the substrate Michaelis constant. The feasibility of module-based T6PP inhibitor design was thus demonstrated. However, two questions remained, which are (i) do T6PP orthologs respond similarly to the inhibitors and (ii) how should the phenyl group be tailored for inhibitor optimization?

Because the T6PP orthologs targeted for the development of therapeutics derive from evolutionarily distant organisms (bacteria, fungi and nematodes) and thus have structures that have diverged a great deal, they are likely to present different and unpredictable profiles for inhibitor recognition. Therefore, we expanded our analysis of the structural determinants of **9a** and Bm-T6PP association by adding T6PP orthologs from *Ascaris suum* (As-T6PP), *Mycobacterium tuberculosis* (Mt-T6PP), *Shigella boydii* (Sb-T6PP) and *Salmonella typhimurium* (St-T6PP). This effort provided a more comprehensive picture of T6PP inhibition. Unfortunately, the group did not include the recently reported fungal T6PP orthologs [20]. The K_i values measured for the *p*-octylphenyl (**9a**) and *p*-hexylphenyl (**9b**) glucopyranoside 6-sulfate inhibitors with the panel of five T6PP orthologs are listed along with the T6P K_m values in Table 1. It is evident that the pattern of inhibitor recognition is somewhat different for each enzyme, underscoring the importance of using the panel of enzymes to evaluate inhibitor-binding strength and ultimately to identify the structural determinants of tight binding.

Through screening T6PP inhibition by members of the assembled library of aryl D-glucopyranoside 6-sulfate (and related) compounds (Fig. 3), we were able to scrutinize the design strategy used in constructing the lead inhibitor **9a**. Each inhibitor was tested (at a concentration of 1 mM) for inhibition of the T6PP orthologs by separately measuring the initial velocities of T6PP-catalyzed hydrolysis at half saturation ([T6P] = K_m) in the presence (V_I) and absence (V) of the inhibitor. The V_I/V values given in Table 2 reflect the fraction of enzyme that is not bound with the inhibitor. Under these conditions $V_I/V = 0.5$ would correspond to a $K_i = 2K_m$ or 0.4–1.4 mM for this group of T6PP orthologs. Therefore, inhibition by substances possessing K_i values as high as 2 mM are detected. For calibration purposes, the T6PP inhibitors trehalose ($K_i > 10$ mM) and T6S (K_i = 50 μM (As-T6PP), 80 μM (Bm-T6PP), 130 μM (Mt-T6PP), 180 μM (St-T6PP) and 330 μM (Sb-T6PP) [19,28]) were included in the screen.

Firstly, we prepared and tested the β-1-*O*-benzylsulfate (**3**) and β-1-*N*-phenylsulfamide (**4**) derivatives of D-glucose to determine whether an alternate strategy, wherein a benzylsulfate (or sulfamide) group replaces the glucose 6-phosphate moiety, might also be used for inhibitor design. However, neither **3** nor **4** displayed inhibition with the T6PP orthologs (an exception being the weak Bm-T6PP inhibition observed with **3**) (Table 2). An inspection of the recent X-ray structures of T6PP bound with T6P [20,21] provides insight into why the glucose-sulfate is better suited for the glucose-phosphate binding site than is benzylsulfate. Specifically, the C2, C3 and C4 OH functions of the glucose 6-sulfate moiety in **T6S** are expected to form hydrogen bonds with the Glu-Lys-Glu triad of the cap domain like those observed for C2, C3 and C4 OH functions in the inner glucosyl moiety of the substrate T6P (see Fig. 2).

Secondly, we determined if the *O*-phenyl group at C1 of the glucose 6-sulfate template is the best option. Thus, the 1-*O*-methyl (**5b**), *O*-(n-octyl) (**6b**), *O*-benzyl (**6a**), *O*-naphthyl (**6c**) *O*-biphenyl (**8b**) and *O*-phenyl-triazole (**2d** and **6d**) derivatives were prepared and screened as were the 1-*N*-phenyl (**2b**) and *N*-phenyl-thiocarbamoyl (**2c**) derivatives (Table 2). The benzyl derivative (**6a** K_i = 160 ± 20 μM) proved to be a more potent inhibitor than the phenyl analog (**5c** K_i = 320 ± 30 μM) towards Bm-T6PP, and but to have comparable potency to that of the phenyl derivative towards the other T6PP orthologs. The *O*-methyl adduct **5b** showed no inhibition, and inhibition by the *O*-(n-octyl) **6b** derivative was weak or absent. Substances containing the larger aryl groups, *O*-naphthyl (**6c**), *O*-biphenyl (**8b**) and *O*-phenyl-triazole (**6d**) do not display significant inhibition, with the exception of the modest inhibition observed for **6c** and **8b** toward Bm-T6PP.

Next, we compared the effectiveness of the *O*-benzyl group at enhancing inhibitor binding affinity when it is located at the glucosyl C2 (**5d**), C3 (**5e**) or C4 (**5f**) position. The relatively strong inhibition conveyed by the 1-*O*-benzyl group (**6a**) towards the Bm-T6PP is attenuated in these analogs and the modest inhibition conveyed by the 1-*O*-benzyl group towards St-T6PP and Sb-T6PP is lost. These findings demonstrate that attachment of an *O*-benzyl or *O*-phenyl group to C1 of the glucosyl moiety is optimal.

Finally, a brief survey of the impact of polar ring substituents on

the *O*-phenyl group at C1 was carried out. In one group of substances prepared for this purpose, the *ortho*, *meta* and *para* phenyl ring positions contain a formyl (**8h**, **8i**, **8j**) and a hydroxymethyl group (**8k**, **8l**, **8m**). In another group, nitro, amino and *N*-acetyl moieties are present at the *para* phenyl ring position (**8e**, **8f** and **8g**). Also, the impact of multi-functionalization was tested using substances containing a combination of 2,3-dimethoxy-4-formyl groups (**8c**) or two fluoride substituents (**8d**). The results show that the formyl substituent has no impact, the hydroxymethyl substituent increases inhibition but only to a small degree, and the amino, nitro, *N*-acetyl and fluoro substituents have only a slight or no impact on inhibition. Furthermore, the multiple ring substituents in **8c** do not result in increased binding affinity.

2.3. Inhibition specificity

The specificity of T6PP inhibitor **9a** was explored using other HAD phosphatases which, unlike T6PP, are promiscuous in their activity with phosphorylated carbohydrate metabolites and, as a result, are predisposed to off-target inhibition. The phosphatases were selected include (i) *E. coli* Ybiv [31], which hydrolyzes a wide variety of phosphates, including glucose 6-, imido-di-, fructose 1-, ribose 5-, acetyl-, glycerol 1- and glycerol 2-phosphate, (ii) *Bacteroides thetaiotaomicron* BT1713 [32], a phosphatase that hydrolyzes in addition to its physiological 2-keto-3-deoxy-D-glycero-D-galacto 9-phosphonononic acid (KDN-9-P), 2-keto-3-deoxy-8-phospho-*d*-manno-octulosonic acid (KDO-8-P), *N*-acetylneuraminate 9-phosphate (Neu5Ac-9-P), pNPP, phosphoenol-pyruvate, and glucose 6-phosphate, tyrosine-phosphate and gluconate 6-phosphate and (iii) *Pseudomonas putida* KT2440 GmhB (D-glycero-β-D-manno-heptose-1,7-bisphosphate 7-phosphatase) [33], which hydrolyzes a variety of hexose and heptose bisphosphate metabolites in addition to its physiological substrate D-glycero-β-D-manno-heptose-1,7-bisphosphate. As the data in Table S2 (Supplementary Information) show, when used at a concentration of 200 μM in the presence of the respective substrates at limiting concentrations (equal to $1/3K_m$), **9a** does not inhibit any of the three HAD phosphatases tested. We infer from this result that **9a** is not a promiscuous inhibitor towards HAD phosphatases, including ones that like T6PP bind and hydrolyze phosphorylated carbohydrate metabolites, but that unlike T6PP, have lax substrate specificities.

3. Conclusion

Taken together, our findings validate the aryl D-glucopyranoside 6-sulfate template as a promising platform to use in combination with T6PP X-ray structures for the construction of potent second-generation inhibitors. We have identified the phenyl group and the benzyl group as superior in the role of the aryl group. A brief survey of phenyl ring substituents showed that small polar ones have little to no impact on binding affinity whereas the long and flexible nonpolar substituents enhance binding. Future inhibitor designs will focus on optimizing binding affinity for target orthologs and on creating active site-directed irreversible inhibitors.

4. Experimental

4.1. General

The structures of the inhibitors selected for this study are given in Fig. 3. Among members of this family, phenyl α-D-glucopyranoside (**1**) and phenyl β-D-glucopyranoside (**2a**) and octyl β-D-glucopyranoside are commercially available substances and glucose derivatives **2b** [34], **2c** [35], **2d** [36], **4** [37], glucose 6-sulfate **5a** [38], **10** [39], along with trehalose 6-phosphatate (**T6P**) [40] and trehalose 6-sulfate (**T6S**) [19,28] were synthesized by using known procedures. The routes utilized for preparation of the other members of the T6PP inhibitor library are displayed in Schemes 1–9 and described in the Experimental section. Either commercially available or previously synthesized aryl β- and α-D-glucopyranosides were employed as starting materials in most of these sequences (Schemes 2–4). In certain cases, the starting materials were previously unknown substances. Accordingly, 3-sulfatomethylphenyl glucoside **11** was prepared from the known aldehyde **10** [39] (Scheme 1). In addition, aryl glucopyranosides **12**–**14** and **16** (Scheme 6) were prepared from 2,3,4,6-tetra-*O*-acetyl-α-D-glucopyranosyl bromide, and **17**–**20** (Scheme 9) were prepared from 1,2,3,4,6-penta-*O*-benzoyl-D-glucopyranose by reaction with the appropriate phenol followed by chromatography on silica gel to separate the β and α anomers. Finally, phenyl β-D-glucopyranoside 6-phosphate (**7**) was produced starting with commercially available phenyl β-D-glucopyranoside (**2a**) (Scheme 5). All synthetic substances were shown to be >95% pure by using NMR spectroscopy and HPLC analysis.

Except where specified, all solvents and reagents were purchased and used without further purification. Analytical thin-layer chromatography (TLC) was performed on silica gel plates containing F_{254} fluorescence indicator and column chromatography was performed using the indicated eluants on silica gel (230–400 mesh). ^{1}H (300 and 500 MHz), ^{13}C NMR (75 MHz and 125 MHz), and ^{31}P (121.5 MHz) NMR spectra were recorded on Bruker Avance 500 and Bruker Avance III 300 spectrometers. ^{1}H and ^{13}C NMR chemical shifts are reported in parts per million (δ) relative to tetramethylsilane (TMS; 0.00 ppm) or solvent peaks as the internal reference, multiplicities are given as s = singlet, d = doublet, t = triplet, q = quartet, m = multiplet, and coupling constant (J) are in Hz; ^{31}P NMR chemical shifts are reported in ppm relative to 50% aq H_3PO_4 as a standard.

4.1.1. 3-Sulfatomethylphenyl β-D-glucopyranoside (3)

A solution of 3-formylphenyl 2,3,4,6-tetra-*O*-acetyl-β-D-glucopyranoside (**10**) (0.976 g, 2.2 mmol) in 50 mL of a 1:1 mixture of THF/EtOH containing $NaBH_4$ (42 mg, 1.1 mmol) was stirred at r.t. until complete disappearance of starting material occurred (TLC). The mixture was poured into ice-water, the pH was adjusted to 7.0 and extracted with chloroform. The extracts were dried and concentrated in vacuo, giving a residue that was dissolved in anhydrous DMF (4 mL). To this solution at −20 °C was added a solution of SO_3.pyridine (0.7 g, 4.4 mmol) in 2 mL anhydrous DMF.

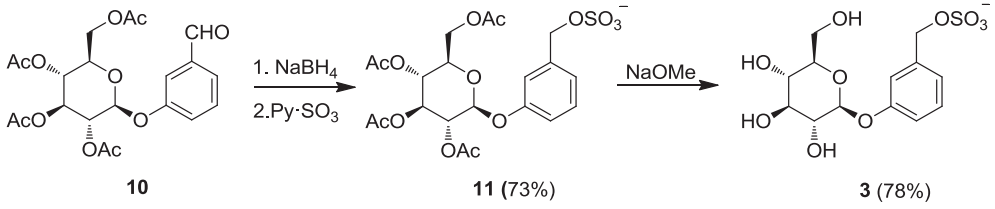

10 **11** (73%) **3** (78%)

Scheme 1. Synthesis of **3**.

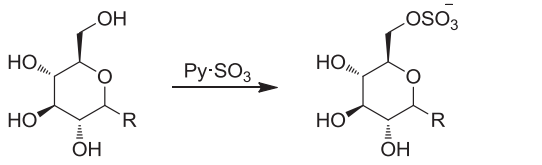

Scheme 2. Synthesis of **5b**, **5c, 6a** and **6d**.

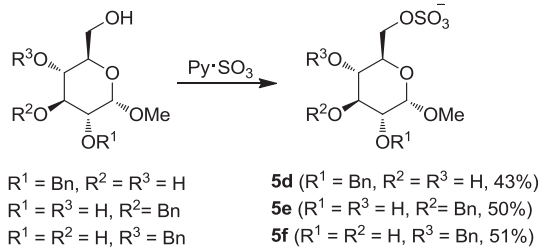

Scheme 3. Synthesis of **5d**, **5e** and **5f**.

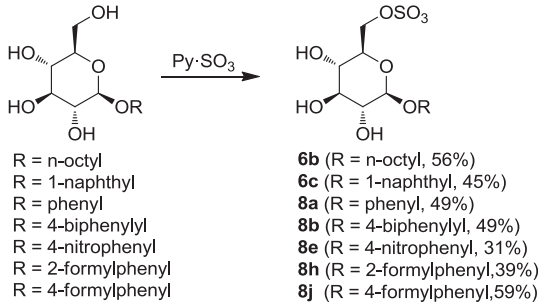

Scheme 4. Synthesis of **6b**, **6c**, **8a**, **8b**, **8e**, **8h** and **8j**.

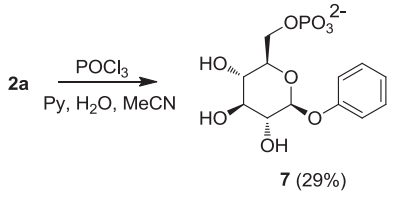

Scheme 5. Synthesis of **7**.

The resulting solution was stirred at r.t. for 12 h and concentrated in vacuo, giving a residue that was subjected to silica gel chromatograph (10:1 to 5:1 DCM/MeOH) to give 3-sulfatomethylphenyl 2,3,4,6-tetra-*O*-acetyl-β-D-glucopyranoside (**11**) (0.857 g, 73%). **^{1}H NMR** (300 MHz, $CDCl_3$) δ (ppm) 7.14 (t, J = 8.1 Hz, 1H), 6.98–6.96 (m, 2H), 6.82–6.79 (m, 1H), 5.22–5.00 (m, 4H), 4.91 (s, 2H), 4.18 (dd, J_1 = 12.6 Hz, J_2 = 5.4 Hz, 1H), 4.07–4.02 (m, 1H), 3.85–3.79 (m, 1H), 1.95 (s, 3H), 1.93 (s, 3H), 1.92 (s, 3H), 1.91 (s, 3H). **^{13}C NMR** (75 MHz, $CDCl_3$) δ (ppm) 170.4, 169.9, 169.3, 169.2, 156.6, 138.5, 129.3, 122.7, 116.4, 116.0, 98.6, 72.5, 71.7, 70.9, 68.9, 68.0, 61.7, 20.5, 20.5, 20.4.

Following addition of sodium (38 mg, 1.64 mmol) to 70 mL of anhydrous methanol, a solution of **11** (768 mg, 1.6 mmol) in anhydrous methanol (4.5 mL) was added dropwise. After stirring at r.t. for 2 h, the mixture was neutralized with solid carbon dioxide, and concentrated in vacuo, giving a residue that was subjected to silica gel chromatography to give 0.485 g (78%) of **3**.**^{1}H NMR** (300 MHz, CD_3OD) δ (ppm) 7.30 (t, J = 8.1 Hz, 1H), 7.21–7.20 (m, 1H), 7.10–7.06 (m, 2H), 5.01 (s, 2H), 4.95 (d, J = 6.9 Hz, 1H), 3.93 (dd, J_1 = 12.0 Hz, J_2 = 1.2 Hz, 1H), 3.74 (dd, J_1 = 12.0 Hz, J_2 = 4.5 Hz, 1H), 3.50–3.47 (m, 4H). **^{13}C NMR** (75 MHz, CD_3OD) δ (ppm) 159.1, 139.4, 130.4, 122.8, 117.3, 102.3, 78.0, 77.9, 74.9, 71.3, 70.4, 62.4. **HRMS** (ESI) m/z calcd. for $C_{13}H_{18}O_{10}S$ $[M\text{-}H]^-$ 365.0542, found 365.0535.

4.1.2. Methyl α-D-glucopyranoside-6-sulfate (*5b*)

To a solution of methyl α-D-glucopyranoside (0.58 g, 3.0 mmol) in anhydrous DMF (9 mL) at −20 °C, was added a solution of SO_3.pyridine (0.50 g, 3.15 mmol) in 1 mL anhydrous DMF, The resulting solution was stirred at r.t. for 12 h and concentrated in vacuo, giving a residue that was subjected to silica gel chromatograph to give 0.435 g (50%) of **5b.** **^{1}H NMR** (300 MHz, CD_3OD) δ (ppm) 4.69 (d, J = 3.9 Hz, 1H), 4.29 (dd, J_1 = 10.8 Hz, J_2 = 1.8 Hz, 1H), 4.16 (dd, J_1 = 10.8 Hz, J_2 = 5.7 Hz, 1H), 3.77–3.71 (m, 1H), 3.64 (t, J = 9.2 Hz, 1H), 3.45–3.41 (m, 1H), 3.43 (s, 3H), 3.56–3.33 (m, 1H). **^{13}C NMR** (75 MHz, CD_3OD) δ (ppm) 101.2, 74.9, 73.4, 71.6, 71.53, 68.3, 55.6. **HRMS** (ESI) m/z calcd. for $C_7H_{14}O_9S$ $[M\text{-}H]^-$ 273.0208, found 273.0278.

4.1.3. Phenyl α-D-glucopyranoside-6-sulfate (*5c*)

This substance was prepared starting with phenyl α-D-glucopyranoside (**1**) using the same procedure employed for the preparation of **5b.** Yield 42%. **^{1}H NMR** (500 MHz, CD_3OD) δ (ppm) 7.30–7.27 (m, 2H), 7.16–7.15 (m, 2H), 7.01 (t, J = 7.5 Hz, 1H), 5.45 (d, J = 3.5 Hz, 1H), 4.22 (dd, J_1 = 10.0 Hz, J_2 = 4.0 Hz, 1H), 4.17–4.15 (m, 1H), 3.88 (t, J = 9.5 Hz, 1H), 3.77–3.70 (m, 1H), 3.59 (dd, J_1 = 10.0 Hz, J_2 = 4.0 Hz, 1H), 3.52 (t, J_1 = 10.0 Hz, 1H). **^{13}C NMR** (125 MHz, CD_3OD) δ (ppm) 158.6, 130.5, 123.5, 118.3, 99.4, 74.6, 73.2, 72.5, 71.1, 67.8. **HRMS** (ESI) m/z calcd. for $C_{12}H_{16}O_9S$ $[M\text{-}H]^-$ 335.0407, found 335.0438.

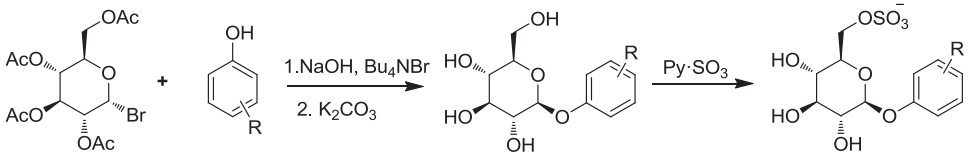

Scheme 6. Synthesis of **8c**, **8d**, **8i** and **8n**.

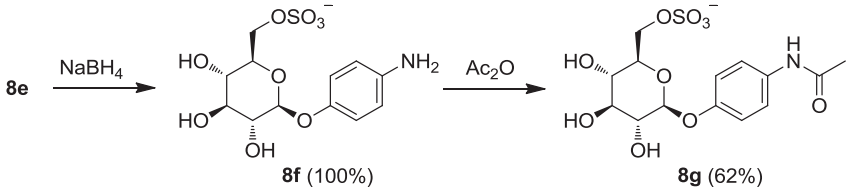

Scheme 7. Synthesis of **8g**.

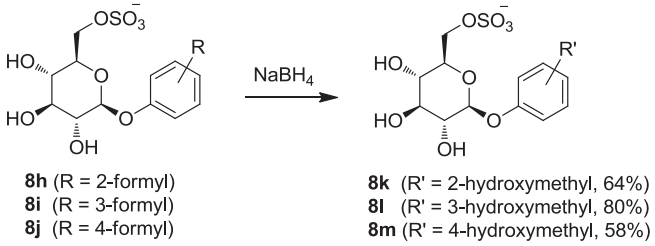

Scheme 8. Synthesis of **8k**, **8l** and **8m**.

*4.1.4. Methyl 2-O-benzyl-α-D-glucopyranoside-6-sulfate (**5d**)*

This substance was prepared starting with methyl 2-*O*-benzyl-α-D-glucopyranoside [41] using the same procedure employed for the preparation of **5b.** Yield 43%. **^{1}H NMR** (300 MHz, CD_3OD) δ (ppm) 7.46–7.41 (m, 2H), 7.40–7.32 (m, 3H), 4.80 (d, J = 12.0 Hz, 1H), 4.68 (d, J = 12.0 Hz, 1H), 4.66 (d, J = 3.9 Hz, 1H), 4.29 (dd, J_1 = 7.8 Hz, J_2 = 2.1 Hz, 1H), 4.17 (dd, J_1 = 10.8 Hz, J_2 = 5.4 Hz, 1H), 3.79 (t, J = 9.3 Hz, 1H), 3.75–3.70 (m, 1H), 3.39–3.37 (m, 1H), 3.37 (s, 3H), 3.36–3.34 (m, 1H). **^{13}C NMR** (75 MHz, CD_3OD) δ (ppm) 139.8, 129.4, 129.2, 128.8, 99.2, 80.9, 74.1, 74.0, 71.6, 71.4, 68.2, 55.5. **HRMS** (ESI) *m/z* calcd. for $C_{14}H_{20}O_9S$ $[M-H]^-$ 363.0750, found 363.0738.

*4.1.5. Methyl 3-O-benzyl-α-D-glucopyranoside-6-sulfate (**5e**)*

This substance was prepared starting with methyl 3-*O*-benzyl-α-D-glucopyranoside [42] using the same procedure employed for the preparation of **5b.** Yield 50%. **^{1}H NMR** (300 MHz, CD_3OD) δ (ppm) 7.44–7.41 (m, 2H), 7.33–7.16 (m, 3H), 4.86 (s, 2H), 4.65 (d, J = 3.6 Hz, 1H), 4.28 (dd, J_1 = 10.8 Hz, J_2 = 1.8 Hz, 1H), 4.16 (dd, J_1 = 10.8 Hz, J_2 = 5.4 Hz, 1H), 3.78–3.72 (m, 1H), 3.62–3.60 (m, 1H), 3.55–3.45 (m, 2H), 3.41 (s, 3H). **^{13}C NMR** (75 MHz, CD_3OD) δ (ppm) 140.5, 129.1, 129.0, 128.4, 101.4, 83.5, 76.2, 73.5, 71.7, 71.4, 68.2, 55.6. **HRMS** (ESI) *m/z* calcd. for $C_7H_{14}O_9S$ $[M-H]^-$ 363.0750, found 363.0739.

*4.1.6. Methyl 4-O-benzyl-α-D-glucopyranoside-6-sulfate (**5f**)*

This substance was prepared starting with methyl 4-*O*-benzyl-α-D-glucopyranoside [43] using the same procedure employed for the preparation of **5b**. Yield 51%. **^{1}H NMR** (500 MHz, CD_3OD) δ (ppm) 7.44–7.43 (m, 2H), 7.33–7.30 (m, 2H), 7.27–7.24 (m, 1H), 4.93–4.91 (m, 1H), 4.75 (m, 1H), 4.67 (d, J = 3.5 Hz, 1H), 4.25 (s, 2H), 3.81–3.75 (m, 1H), 3.45–3.43 (m, 2H), 3.40 (s, 3H). **^{13}C NMR** (75 MHz, CD_3OD) δ (ppm) 139.9, 129.4, 129.2, 128.6, 101.2, 79.3, 75.9, 75.5, 73.6, 70.6, 67.8, 55.7. **HRMS** (ESI) *m/z* calcd. for $C_{14}H_{20}O_9S$ $[M-H]^-$ 363.0750, found 363.0740.

*4.1.7. Benzyl α-D-glucopyranoside-6-sulfate (**6a**)*

This substance was prepared from benzyl α-D-glucopyranoside [44] using the same procedure described for the preparation of **5b.** Yield 47%. **^{1}H NMR** (300 MHz, CD_3OD) δ (ppm) 7.45–7.43 (m, 2H), 7.34–7.30 (m, 3H), 4.88 (d, J = 3.6 Hz, 1H), 4.77 (d, J = 11.7 Hz, 1H), 4.56 (d, J = 11.7 Hz, 1H), 4.26 (dd, J_1 = 10.8 Hz, J_2 = 3.8 Hz, 1H), 4.15 (dd, J_1 = 10.8 Hz, J_2 = 5.4 Hz, 1H), 3.83–3.80 (m, 1H), 3.72 (t, J = 9.3 Hz, 1H), 3.46–3.37 (m, 2H). **^{13}C NMR** (75 MHz, CD_3OD) δ (ppm) 138.7, 129.3, 129.2, 128.7, 99.1, 74.7, 73.2, 71.8, 71.4, 70.3, 62.1. **HRMS** (ESI) *m/z* calcd. for $C_{13}H_{18}O_9S$ $[M-H]^-$ 349.0593, found 349.0585.

*4.1.8. n-Octyl β-D-glucopyranoside-6-sulfate (**6b**)*

This substance was prepared starting with n-octyl β-D-glucopyranoside using the same procedure described for the preparation of **5b.** Yield 56%. **^{1}H NMR** (300 MHz, CD_3OD) δ (ppm) 4.33–4.23 (m, 2H), 4.13 (dd, J_1 = 11.1 Hz, J_2 = 5.6 Hz, 1H), 3.90–3.83 (m, 1H), 3.56–3.44 (m, 2H), 3.38–3.33 (m, 2H), 3.18 (t, J = 7.2 Hz, 1H), 1.64–1.56 (m, 2H), 1.38–1.26 (m, 10H), 0.90 (t, J = 6.6 Hz, 3H). **^{13}C**

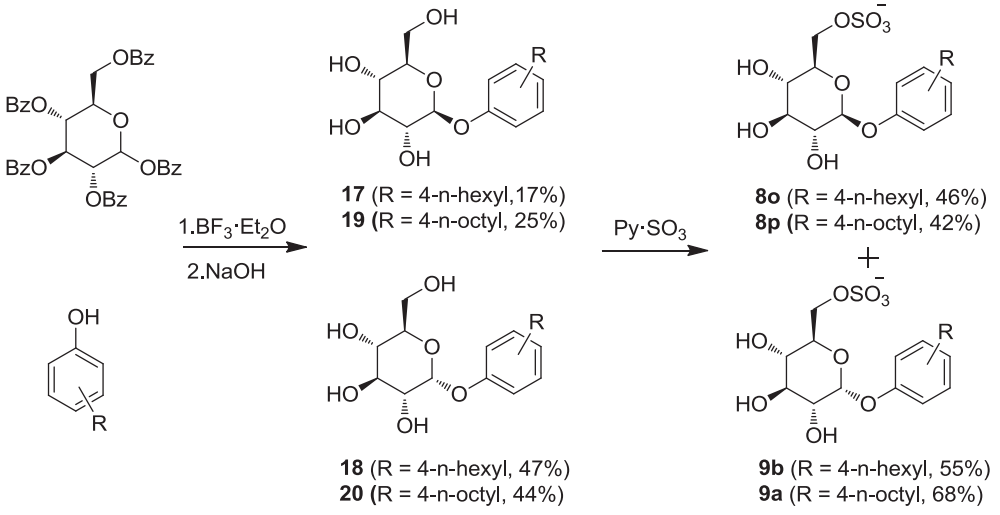

Scheme 9. Synthesis of **8o**, **8p**, **9a** and **9b**.

NMR (75 MHz, CD_3OD) δ (ppm) 104.3, 77.7, 75.9, 75.0, 71.4, 71.0, 68.2, 33.0, 30.8, 30.6, 30.4, 27.1, 23.7, 14.4. **HRMS** (ESI) *m/z* calcd. for $C_{14}H_{28}O_9S$ $[M-H]^-$ 371.1376, found 371.1373.

4.1.9. 1-Naphthyl β-D-glucopyranoside-6-sulfate (**6c**)

This substance was prepared starting with 1-naphthyl β-D-glucopyranoside (purchased from Carbosynth Limited) using the same procedure described for the preparation of **5b.** Yield 45%. **^{1}H NMR** (500 MHz, CD_3OD) δ (ppm) 8.38–8.36 (m, 1H), 7.79–7.77 (m, 1H), 7.50–7.44 (m, 3H), 7.40–7.37 (m, 1H), 7.24–7.22 (m, 1H), 5.10 (d, J = 7.5 Hz, 1H), 4.39 (m, 1H), 4.21 (dd, J_1 = 11.0 Hz, J_2 = 5.5 Hz, 1H), 3.77–3.67 (m, 2H), 3.59–3.50 (m, 2H). **^{13}C NMR** (125 MHz, CD_3OD) δ (ppm) 154.4, 135.8, 128.4, 127.3, 127.1, 127.0, 126.3, 123.2, 123.0, 110.6, 102.6, 77.7, 75.9, 75.0, 71.2, 68.1. **HRMS** (ESI) *m/z* calcd. for $C_{16}H_{18}O_9S$ $[M-H]^-$ 385.0593, found 385.0589.

4.1.10. (4-Phenyl-1H-1,2,3-triazol-1-yl) β-D-glucopyranoside-6-sulfate (**6d**)

This substance was prepared starting with **2d** using the same procedure described for the preparation of **5b.** Yield 55%. **^{1}H NMR** (300 MHz, D_2O) δ (ppm) 8.35 (s, 1H), 7.68–7.65 (m, 2H), 7.46–7.42 (m, 3H), 5.74 (d, J = 9.0 Hz, 1H), 4.47–4.43 (m, 1H), 4.37–4.35 (m, 1H), 4.05–4.02 (m, 2H), 3.78–3.74 (m, 2H), **^{13}C NMR** (75 MHz, D_2O) δ (ppm) 147.5, 129.0, 128.9, 125.6, 121.0, 87.4, 76.7, 75.7, 75.3, 72.2, 68.8. **HRMS** (ESI) *m/z* calcd. for $C_{14}H_{17}N_3O_8S$ $[M-H]^-$ 386.0664, found 386.0666.

4.1.11. Phenyl β-D-glucopyranoside-6-phosphate (**7**)

To a solution of phenyl β-D-glucopyranoside (**2a**) (1.08 g, 4.0 mmol) in 5.08 mL of a 2.5:1:0.1 mixture of acetonitrile/pyridine/water at 0 °C was added $POCl_3$ (1.6 mL, 8 mmol). The resulting solution was stirred at 0 °C for 2 h and poured onto 20 g of ice. After the ice melted, the pH of the mixture was adjusted to 7.0 by slowly adding 1 M aqueous NaOH. The resulting solution was concentrated in vacuo, giving a residue that was subjected to silica gel chromatograph (ethyl acetate/isopropyl alcohol/H_2O/$NH_3 \cdot H_2O$ = 5/5/2/0.2, v/v/v/v) to give **7** (0.38 g, 29%). **^{1}H NMR** (300 MHz, D_2O) δ (ppm) 7.42–7.37 (m, 2H), 7.16–7.12 (m, 3H), 5.13 (d, J = 7.2 Hz, 1H), 4.08–4.06 (m, 2H), 3.68–3.59 (m, 4H). **^{13}C NMR** (75 MHz, D_2O) δ (ppm) 156.5, 129.9, 123.3, 116.5, 100.2, 75.3, 75.1, 73.0, 68.7, 62.8.**^{31}P NMR** (121.5 MHz, D_2O) δ (ppm) 3.32. **HRMS** (ESI) *m/z* calcd. for $C_{12}H_{17}O_9P$ $[M-H]^-$ 335.0532, found 335.0529.

4.1.12. Phenyl β-D-glucopyranoside-6-sulfate (**8a**)

This substance was prepared using starting with **2a** using the same procedure described for the preparation of **5b.** Yield 49%. **^{1}H NMR** (300 MHz, CD_3OD) δ (ppm) 7.32–7.27 (m, 2H), 7.13–7.10 (m, 2H), 7.04–6.99 (m, 1H), 4.90 (d, J = 7.5 Hz, 1H), 4.39 (dd, J_1 = 10.8 Hz, J_2 = 1.4 Hz, 1H), 4.19 (dd, J_1 = 10.8 Hz, J_2 = 5.7 Hz, 1H), 3.69 (t, J = 7.4 Hz, 1H), 3.51–3.48 (m, 3H). **^{13}C NMR** (75 MHz, CD_3OD) δ (ppm) 159.1, 130.4, 123.4, 117.8, 102.3, 77.6, 75.9, 74.8, 71.2, 68.1. **HRMS** (ESI) *m/z* calcd. for $C_{12}H_{16}O_9S$ $[M-H]^-$ 335.0437, found 335.0429.

4.1.13. 4-Biphenylyl β-D-glucopyranoside-6-sulfate (**8b**)

This substance was prepared starting with 4,4'-biphenyl β-D-glucopyranoside [45] using the same procedure described for the preparation of **5b.** Yield 49%. **^{1}H NMR** (500 MHz, CD_3OD) δ (ppm) 7.54–7.51 (m, 4H), 7.38–7.34 (m, 2H), 7.26–7.23 (m, 1H), 7.16–7.15 (m, 2H), 4.90 (d, J = 7.0 Hz, 1H), 4.37 (m, 1H), 4.14 (dd, J_1 = 11.0 Hz, J_2 = 6.0 Hz, 1H), 3.68 (t, J = 7.3 Hz, 1H), 3.50–3.40 (m, 3H). **^{13}C NMR** (125 MHz, CD_3OD) δ (ppm) 158.6, 142.0, 136.7, 129.8, 129.0, 127.6, 118.2, 102.4, 77.7, 76.1, 74.9, 71.3, 68.2. **HRMS** (ESI) *m/z* calcd. for $C_{18}H_{20}O_9S$ $[M-H]^-$ 411.0705, found 411.0746.

4.1.14. 2,6-Dimethoxy-4-formylphenyl β-D-glucopyranoside-6-sulfate (**8c**)

To a solution of 2,3,4,6-tetra-*O*-acetyl-α-D-glucopyranosyl bromide (0.824 g, 2 mmol) in CH_2Cl_2 (8 mL), containing tetrabutylammonium bromide (0.76 g, 2 mmol) and syringaldehyde (1.09 g, 6 mmol) was added 8 mL of 1 M NaOH. The resulting mixture was stirred vigorously at 35 °C for 6 h. The mixture was diluted with EtOAc and the organic phase was separated, washed three times with a 1 M NaOH aqueous solution, water and brine, dried and concentrated in vacuo. The resulting residue was dissolved in 20 mL of a 1:1 mixture of THF/MeOH containing anhydrous K_2CO_3 (0.5 g). The resulting mixture was stirred for 20 h at r.t. and concentrated in vacuo, giving a residue that was subjected to silica gel chromatography to give 2,6-dimethoxy-4-formylphenyl β-D-glucopyranoside (**12**) [46] (364 mg, 53%). **^{1}H NMR** (300 MHz, CD_3OD/D_2O (v/v, 1/2)) δ (ppm) 9.91 (s, 1H), 7.39 (s, 2H), 5.24 (d, J = 7.2 Hz, 1H), 4.02 (s, 6H), 3.87–3.78 (m, 2H), 3.65–3.58 (m, 3H), 3.42–3.39 (m, 1H). **^{13}C NMR** (75 MHz, CD_3OD/D_2O (v/v, 1/2)) δ (ppm) 195.0, 154.2, 140.6, 133.6, 108.4, 103.8, 77.7, 77.0, 74.9, 70.4, 61.6, 57.2.

The target **8c** was prepared from **12** using the same procedure as described for the preparation of **5b.** Yield 58%. **^{1}H NMR** (300 MHz, D_2O) δ (ppm) 9.44 (s, 1H), 6.90 (s, 2H), 5.07 (d, J = 5.7 Hz, 1H), 4.30–4.18 (m, 2H), 3.82 (s, 6H), 3.64–3.60 (m, 4H). **^{13}C NMR** (75 MHz, D_2O) δ (ppm) 194.3, 152.6, 138.8, 132.1, 107.1, 102.7, 75.4, 74.1, 73.5, 69.1, 66.8, 56.1. **HRMS** (ESI) *m/z* calcd. for $C_{15}H_{20}O_{12}S$ $[M-H]^-$ 423.0597, found 423.0599.

4.1.15. 3,4-Difuorophenyl β-D-glucopyranoside-6-sulfate (**8d**)

3,4-Difuorophenyl β-D-glucopyranoside (**13**) was prepared using the same procedure as that for 2,6-dimethoxy-4-formylphenyl β-D-glucopyranoside (**12**). Yield 45%. **^{1}H NMR** (300 MHz, D_2O) δ (ppm) 7.14–7.04 (m, 1H), 7.01–6.94 (m, 1H), 6.85–6.81 (m, 1H), 4.77 (d, J = 5.1 Hz, 1H), 3.83 (dd, J_1 = 12.0 Hz, J_2 = 2.0 Hz, 1H), 3.63 (dd, J_1 = 12.0 Hz, J_2 = 5.4 Hz, 1H), 3.45–3.31 (m, 4H). **^{13}C NMR** (75 MHz, CD_3OD) δ (ppm) 155.4 (d, $J_{C,F}$ = 6.6 Hz), 150.90 (dd, $J_{C,F1}$ = 319.1 Hz, $J_{C,F2}$ = 13.7 Hz), 147.8 (dd, $J_{C,F1}$ = 313.8 Hz, $J_{C,F2}$ = 14.0 Hz), 118.2 (d, $J_{C,F}$ = 18.7 Hz), 113.9, 107.6 (d, $J_{C,F}$ = 20.3 Hz), 102.8, 78.1, 77.8, 74.1, 71.2, 62.4.

The target **8d** was prepared from **13** using the same procedure as that for **5b.** Yield 33%. **^{1}H NMR** (300 MHz, CD_3OD) δ (ppm) 7.10–7.01 (m, 1H), 6.94–6.92 (m, 1H), 6.86–6.79 (m, 1H), 4.45 (d, J = 10.8 Hz, 1H), 4.29–0.20 (m, 1H), 4.03–3.82 (m, 2H), 3.65 (t, J = 9.0 Hz, 1H), 3.53–3.38 (m, 2H). **^{13}C NMR** (75 MHz, CD_3OD) δ (ppm) 155.2 (d, $J_{C,F}$ = 4.7 Hz), 150.9 (dd, $J_{C,F1}$ = 298.4 Hz, $J_{C,F2}$ = 4.7 Hz), 147.74 (dd, $J_{C,F1}$ = 312.2 Hz, $J_{C,F2}$ = 12.8 Hz), 118.3 (d, $J_{C,F}$ = 18.8 Hz), 113.9, 107.8 (d, $J_{C,F}$ = 19.2 Hz), 102.4, 75.8, 75.5, 73.5, 70.0, 68.0. **HRMS** (ESI) *m/z* calcd. for $C_{12}H_{14}F_2O_9S$ $[M-H]^-$ 371.0248, found 371.0239.

4.1.16. 4-Nitrophenyl β-D-glucopyranoside-6-sulfate (**8e**)

This substance was prepared using the same procedure as that for **5b** starting with 4-nitrophenyl β-D-glucopyranoside [47]. Yield 31%. **^{1}H NMR** (300 MHz, CD_3OD) δ (ppm) 8.19 (d, J = 9.3 Hz, 2H), 7.24 (d, J = 9.3 Hz, 2H), 5.08 (d, J = 7.2 Hz, 1H), 3.40 (dd, J_1 = 11.1 Hz, J_2 = 1.8 Hz, 1H), 4.17 (dd, J_1 = 11.1 Hz, J_2 = 6.0 Hz, 1H), 3.85–3.80 (m, 1H), 3.57–3.47 (m, 3H). **^{13}C NMR** (75 MHz, CD_3OD) δ (ppm) 163.6, 143.7, 126.6, 117.7, 101.3, 77.3, 75.9, 74.5, 71.0, 68.0. **HRMS** (ESI) *m/z* calcd. for $C_{12}H_{15}NO_{11}S$ $[M-H]^-$ 380.0288, found 380.0284.

4.1.17. 4-Aminophenyl β-D-glucopyranoside-6-sulfate (**8f**) [48]

To a solution of **8e** (120 mg, 0.3 mmol) in DI water (6 mL), was added $Pd(OH)_2/C$ (32 mg, 0.06 mmol). The resulting mixture was stirred under a H_2 atmosphere for 2 h. The mixture was filtered through Celite pad and the filtrate was concentrated in vacuo, giving **8f** (105 mg, 100%). **^{1}H NMR** (500 MHz, D_2O) δ (ppm)

7.06–7.03 (m, 2H), 6.91–6.88 (m, 2H), 4.98 (d, J = 8.0 Hz, 1H), 4.38–4.35 (m, 1H), 4.29–4.26 (m, 1H), 3.82–3.80 (m, 1H), 3.63–3.55 (m, 3H). **^{13}C NMR** (125 MHz, D_2O) δ (ppm) 143.9, 132.4111.3, 111.0, 94.2, 68.3, 66.6, 65.8, 62.0, 59.7. **HRMS** (ESI) m/z calcd. for $C_{12}H_{17}NO_9S$ $[M-H]^-$ 350.0546, found 350.0536.

*4.1.18. 4-Acetamidophenyl β-D-glucopyranoside-6-sulfate (**8g**) [48]*

A mixture of **8f** (95 mg, 0.27 mmol) in 4.5 mL H_2O containing K_2CO_3 (112 mg, 0.81 mmol) was stirred at 0 °C before adding Ac_2O (77 μL, 0.81 mmol) dropwise. Following stirring at for 3 h at 0 °C, the mixture was concentrated in vacuo, giving a residue that was subjected to silica gel chromatography, to give **8g** (65 mg, 62%). **^{1}H NMR** (300 MHz, D_2O) δ (ppm) 7.34 (d, J = 8.7 Hz, 2H), 7.13 (d, J = 8.7 Hz, 2H), 5.08 (d, J = 7.2 Hz, 1H), 4.38–4.35 (m, 1H), 4.23 (dd, J_1 = 11.4 Hz, J_2 = 5.4, 1H), 3.87–3.83 (m, 1H), 3.62–3.56 (m, 3H), 2.13 (s, 3H). **^{13}C NMR** (75 MHz, D_2O) δ (ppm) 172.9, 154.1, 132.0, 123.9, 117.1, 100.5, 75.3, 73.9, 72.8, 69.1, 66.8, 22.6. **HRMS** (ESI) m/z calcd. for $C_{14}H_{19}NO_{10}S$ $[M-H]^-$ 392.0651, found 392.0645.

*4.1.19. 2-Formylphenyl β-D-glucopyranoside-6-sulfate (**8h**)*

This substance was prepared using the same procedure as that for **5b** starting with 2-formylphenyl β-D-glucopyranoside [49]. Yield 39%. **^{1}H NMR** (500 MHz, D_2O) δ (ppm) 10.03 (s, 1H), 7.72–7.64 (m, 2H), 7.27–7.17 (m, 2H), 5.20 (d, J = 7.5 Hz, 1H), 4.38–4.35 (m, 1H), 4.26–4.23 (m, 1H), 3.87–3.86 (m, 1H), 3.69–3.58 (m, 3H). **^{13}C NMR** (125 MHz, D_2O) δ (ppm) 186.1, 151.9, 130.2, 121.4, 117.6, 116.1, 108.7, 92.8, 68.3, 66.9, 65.6, 61.9, 59.7. **HRMS** (ESI) m/z calcd. for $C_{13}H_{16}O_{10}S$ $[M-H]^-$ 363.0386, found 363.0379.

*4.1.20. 3-Formylphenyl β-D-glucopyranoside-6-sulfate (**8i**)*

3-Formylphenyl β-D-glucopyranoside (**14**) was prepared from 3-hydroxybenzaldehyde and 2,3,4,6-tetra-*O*-acetylglucosyl bromide using the same procedure as that for **12.** Yield 29%. **^{1}H NMR** (300 MHz, CD_3OD) δ (ppm) 9.88 (s, 1H), 7.54–7.34 (m, 4H), 4.96 (d, J = 6.3 Hz, 1H), 3.88–3.84 (m, 1H), 3.67 (dd, J_1 = 12.0 Hz, J_2 = 5.1 Hz, 1H), 3.48–3.39 (m, 4H). **^{13}C NMR** (75 MHz, CD_3OD) δ (ppm) 193.9, 159.5, 139.2, 131.3, 125.0, 124.1, 117.7, 102.0, 78.1, 77.8, 74.7, 71.2, 62.3.

The target **8i** was prepared from **14** substance was prepared using the same procedure as that for **5b.** Yield 39%. **^{1}H NMR** (300 MHz, D_2O) δ (ppm) 9.83 (s, 1H), 7.63–7.49 (m, 3H), 7.41–7.37 (m, 1H), 5.14 (d, J = 6.6 Hz, 1H), 4.33–4.29 (m, 1H), 4.15 (dd, J_1 = 11.4 Hz, J_2 = 5.7 Hz, 1H), 3.87–3.82 (m, 1H), 3.58–3.50 (m, 3H). **^{13}C NMR** (125 MHz, D_2O) δ (ppm) 188.6, 149.8, 130.1, 123.6, 118.0, 116.4, 109.6, 92.9, 68.2, 66.8, 65.6, 61.9, 59.7. **HRMS** (ESI) m/z calcd. for $C_{13}H_{16}O_{10}S$ $[M-H]^-$ 363.0386, found 363.0384.

*4.1.21. 4-Formylphenyl β-D-glucopyranoside-6-sulfate (**8j**)*

The precursor 4-Formylphenyl β-D-glucopyranoside (**15**) was synthesized by using a previously described procedure [50]. The target **8j** was prepared starting with **15** using the same procedure as that for **5b.** Yield 59%. **^{1}H NMR** (300 MHz, D_2O) δ (ppm) 9.81 (s, 1H), 7.93 (d, J = 8.7 Hz, 2H), 7.27 (d, J = 8.7 Hz, 2H), 5.30 (d, J = 6.9 Hz, 1H), 4.46–4.43 (m, 1H), 4.31 (dd, J_1 = 11.4 Hz, J_2 = 5.1 Hz, 1H), 4.01–3.97 (m, 1H), 3.73–3.64 (m, 3H). **^{13}C NMR** (75 MHz, D_2O) δ (ppm) 188.5, 155.3, 126.1, 124.3, 110.0, 92.8, 68.8, 67.5, 66.2, 62.6, 60.3. **HRMS** (ESI) m/z calcd. for $C_{13}H_{16}O_{10}S$ $[M-H]^-$ 363.0386, found 363.0381.

*4.1.22. 2-Hydroxymethylphenyl β-D-glucopyranoside-6-sulfate (**8k**)*

To a solution of 2-formylphenyl β-D-glucopyranoside-6-sulfonate (**8h**) (98 mg, 0.26 mmol) in MeOH (2 mL) at 0 °C, was added $NaBH_4$ (40 mg, 1.03 mmol). The mixture was warmed to room temperature and stirred for 1 h, then diluted with water, and concentrated in vacuo giving a residue that was subjected to silica gel chromatography, giving **8k** (61 mg, 64%). **^{1}H NMR** (500 MHz, D_2O) δ (ppm) 7.38–7.35 (m, 2H), 7.22–7.21 (m, 1H), 7.15–7.12 (m, 1H), 5.10 (d, J = 7.5 Hz, 1H), 4.73–4.65 (m, 2H), 4.35–4.32 (m, 1H), 4.23–4.20 (m, 1H), 3.83–3.82 (m, 1H), 3.65–3.55 (m, 3H). **^{13}C NMR** (125 MHz, D_2O) δ (ppm) 122.6, 122.4, 122.2, 116.3, 108.3, 93.5, 68.3, 66.7, 65.7, 61.9, 59.7, 52.1. **HRMS** (ESI) m/z calcd. for $C_{13}H_{18}O_{10}S$ $[M-H]^-$ 365.0548, found 365.0540.

*4.1.23. 3-Hydroxymethylphenyl β-D-glucopyranoside-6-sulfate (**8l**)*

This substance was prepared from 3-formylphenyl β-D-glucopyranoside-6-sulfonate (**8i**) using the same procedure as that for **8k.** Yield 80%. **^{1}H NMR** (500 MHz, D_2O) δ (ppm) 7.37–7.36 (m, 1H), 7.10–7.07 (m, 3H), 5.10 (d, J = 4.5 Hz, 1H), 4.61–4.59 (m, 2H), 4.36–4.34 (m, 1H), 4.20 (dd, J_1 = 11.0 Hz, J_2 = 5.0 Hz, 1H), 3.86–3.85 (m, 1H), 3.61–3.56 (m, 3H). **^{13}C NMR** (125 MHz, D_2O) δ (ppm) 126.2, 123.0, 119.5, 114.9, 108.6, 108.1, 93.1, 68.2, 66.7, 65.7, 62.0, 59.7, 56.4. **HRMS** (ESI) m/z calcd. for $C_{13}H_{18}O_{10}S$ $[M-H]^-$ 365.0548, found 365.0538.

*4.1.24. 4-Hydroxymethylphenyl β-D-glucopyranoside-6-sulfate (**8m**)*

This substance was prepared from 4-formylphenyl β-D-glucopyranoside-6-sulfonate (**8j**) using the same procedure as that for **8k.** Yield 58%. **^{1}H NMR** (500 MHz, D_2O) δ (ppm) 7.35–7.33 (m, 2H), 7.12–7.10 (m, 2H), 5.09 (d, J = 4.5 Hz, 1H), 4.56–4.55 (m, 2H), 4.34–4.32 (m, 1H), 4.22–4.20 (m, 1H), 3.84–3.83 (m, 1H), 3.58–3.54 (m, 3H). **^{13}C NMR** (125 MHz, D_2O) δ (ppm) 149.0, 127.8, 122.1, 109.5, 93.1, 68.2, 66.7, 65.7, 61.9, 59.7, 56.2. **HRMS** (ESI) m/z calcd. for $C_{13}H_{18}O_{10}S$ $[M-H]^-$ 365.0548, found 365.0538.

*4.1.25. 4-n-Butylphenyl β-D-glucopyranoside-6-sulfate (**8n**)*

4-*n*-Butylphenyl β-D-glucopyranoside (**16**) was prepared from 4-*n*-butylphenol using the same procedure as that for **12.** Yield 30% in two steps. **^{1}H NMR** (300 MHz, CD_3OD) δ (ppm) 7.18–7.07 (m, 4H), 4.98 (d, J = 7.2 Hz, 1H), 3.98–3.94 (m, 1H), 3.80 (dd, J_1 = 11.1 Hz, J_2 = 4.5 Hz, 1H), 3.61–3.53 (m, 4H), 2.59 (t, J = 7.7 Hz, 2H), 1.62–1.57 (m, 2H), 1.40–1.33 (m, 2H), 0.96 (t, J = 7.4 Hz, 3H). **^{13}C NMR** (75 MHz, CD_3OD) δ (ppm) 156.6, 138.2, 130.3, 117.6, 102.2, 77.5, 77.3, 74.5, 70.9, 62.1, 35.5, 34.8, 23.0, 14.2.

The target **8n** was prepared from **16** using the same procedure as that for **5b.** Yield 51%. **^{1}H NMR** (300 MHz, D_2O/CD_3OD (v/v, 1/1)) δ (ppm) 7.21–7.06 (m, 4H), 4.99 (d, J = 6.9 Hz, 1H), 4.39–4.35 (m, 1H), 4.24 (dd, J_1 = 11.1 Hz, J_2 = 5.1 Hz, 1H), 3.78–3.77 (m, 1H), 3.59–3.56 (m, 3H), 2.59 (t, J = 7.7 Hz, 2H), 1.63–1.53 (m, 2H), 1.40–1.30 (m, 2H), 0.93 (t, J = 7.4 Hz, 3H). **^{13}C NMR** (75 MHz, D_2O/CD_3OD (v/v, 1/1)) δ (ppm) 156.1, 138.8, 130.4, 117.6, 102.1, 76.7, 75.1, 74.1, 70.4, 67.8, 35.2, 34.4, 22.7, 14.2. **HRMS** (ESI) m/z calcd. for $C_{16}H_{24}O_9S$ $[M-H]^-$ 391.1063, found 391.1075.

*4.1.26. 4-n-Hexylphenyl β-D-glucopyranoside (17) and 4-n-hexylphenyl α-D-glucopyranoside (**18**) [51]*

To a solution of penta-*O*-benzoyl-D-glucose (2.8 g, 4 mmol) and 4-*n*-hexylphenol (1.42 g, 8 mmol) in dichloromethane (28 mL) under argon at 0 °C was added $BF_3 \cdot Et_2O$ (1.67 mL, 13.2 mmol). The mixture was stirred at 50 °C for 48 h, diluted with water (30 mL) and stirred for 15 min. The mixture was diluted with dichloromethane (60 mL), washed with water, brine, and concentrated in vacuo, giving a residue that was dissolved in THF/MeOH (100 mL/20 mL) and cooled to 0 °C. A 3 N solution of aq NaOH (9.52 mL) was added and the mixture was stirred for 9 h at room temperature, diluted with water (40 mL), neutralized with AG 50W-X8 resin (Bio-Rad), filtered, and concentrated in vacuo, giving a residue that was subjected to silica gel chromatography, giving 4-*n*-hexylphenyl β-D-glucopyranoside (**17**) (237 mg, 17%) and 4-*n*-hexylphenyl α-D-

glucopyranoside (**18**) (639 mg, 47%).

17: **^{1}H NMR** (300 MHz, $CDCl_3/CD_3OD$ (v/v, 1/1)) δ (ppm) 7.59–7.45 (m, 4H), 5.39 (d, J = 6.9 Hz, 1H), 4.39–4.26 (m, 2H), 4.06–4.04 (m, 3H), 3.93–3.92 (m, 1H), 3.04 (t, J = 7.7 Hz, 2H), 2.07–2.05 (m, 2H), 1.84–1.79 (m, 6H), 1.38 (t, J = 6.6 Hz, 3H). 13C NMR (75 MHz, CDCl3/CD3OD (v/v, 1/1)) δ (ppm) 155.1, 137.0, 129.0, 116.3, 100.8, 76.1, 75.9, 73.1, 69.4, 61.0, 34.8, 31.4, 31.4, 28.6, 22.3, 13.6.

18: **^{1}H NMR** (300 MHz, $CDCl_3/CD_3OD$ (v/v, 1/1)) δ (ppm) 7.36–7.29 (m, 4H), 5.75 (d, J = 3.6 Hz, 1H), 4.19 (t, J = 9.3 Hz, 1H), 4.10–3.98 (m, 3H), 3.93–3.82 (m, 2H), 2.81 (t, J = 7.7 Hz, 2H), 1.86–1.84 (m, 2H), 1.58–1.57 (m, 6H), 1.56 (t, J = 6.6 Hz, 3H). **^{13}C NMR** (75 MHz, $CDCl_3/CD_3OD$ (v/v, 1/1)) δ (ppm) 154.7, 136.8, 129.0, 116.6, 97.7, 73.4, 72.2, 71.6, 69.3, 60.7, 34.8, 31.4, 31.3, 28.6, 22.3, 13.6.

4.1.27. 4-n-Hexylphenyl β-D-glucopyranoside-6-sulfate (*8o*)

This substance was prepared from 4-*n*-hexylphenyl β-D-glucopyranoside (**17**) using the same procedure as that for **5b**. Yield 46%. **^{1}H NMR** (300 MHz, D_2O/CD_3OD (v/v, 1/1)) δ (ppm) 7.19–7.09 (m, 4H), 4.99 (d, J = 6.6 Hz, 1H), 4.43–4.40 (m, 1H), 4.29 (dd, J_1 = 11.1 Hz, J_2 = 5.4 Hz, 1H), 3.80–3.76 (m, 1H), 3.65–3.57 (m, 3H), 2.60 (t, J = 7.5 Hz, 2H), 1.65–1.60 (m, 2H), 1.38–1.35 (m, 6H), 0.95 (t, J = 6.6 Hz, 3H). **^{13}C NMR** (75 MHz, $CDCl_3/CD_3OD$ (v/v, 1/1)) δ (ppm) 156.6, 138.3, 130.2, 117.7, 102.4, 77.0, 75.4, 74.4, 70.7, 67.9, 35.8, 32.6, 32.5, 29.6, 23.4, 14.4. **HRMS** (ESI) m/z calcd. for $C_{18}H_{28}O_9S$ $[M-H]^-$ 419.1376, found 419.1388.

4.1.28. 4-n-Hexylphenyl α-D-glucopyranoside-6-sulfate (*9b*)

This substance was prepared from 4-*n*-hexylphenyl α-D-glucopyranoside (**18**) using the same procedure as that for **5b.** Yield 55%. **^{1}H NMR** (300 MHz, CD_3OD) δ (ppm) 7.12–7.05 (m, 4H), 5.44 (d, J = 3.6 Hz, 1H), 4.29–4.17 (m, 2H), 3.94–3.88 (m, 2H), 3.65–3.52 (m, 2H), 2.56 (t, J = 7.7 Hz, 2H), 1.61–1.54 (m, 2H), 1.33–1.31 (m, 6H), 0.91 (t, J = 6.6 Hz, 3H). **^{13}C NMR** (75 MHz, CD_3OD) δ (ppm) 156.5, 138.0, 130.2, 118.2, 99.5, 74.5, 73.1, 72.3, 71.1, 67.8, 36.0, 32.8, 29.9, 23.2, 14.4. **HRMS** (ESI) m/z calcd. for $C_{18}H_{28}O_9S$ $[M-H]^-$ 419.1376, found 419.1375.

4.1.29. 4-n-Octylphenyl β-D-glucopyranoside (19) and 4-n-octyl phenyl α-D-glucopyranoside (*20*) [51]

These substances were prepared using the same procedure as those for 4-*n*-hexylphenyl β-D-glucopyranoside (**17**) and 4-*n*-hexylphenyl α-D-glucopyranoside (**18**).

19: Yield 25%. **^{1}H NMR** (300 MHz, CD_3OD) δ (ppm) 7.03–6.92 (m, 4H), 4.80 (d, J = 6.6 Hz, 1H), 3.84–3.80 (m, 1H), 3.64 (dd, J_1 = 11.4 Hz, J_2 = 3.6 Hz, 1H), 3.40–3.35 (m, 4H), 2.47 (t, J = 7.5 Hz, 2H), 1.54–1.48 (m, 2H), 1.24–1.23 (m, 10H), 0.83 (t, J = 6.3 Hz, 3H). **^{13}C NMR** (75 MHz, CD_3OD) δ (ppm) 157.2, 137.9, 130.2, 117.7, 102.5, 78.0, 77.9, 74.9, 71.3, 62.5, 36.1, 33.0, 32.9, 30.6, 30.4, 30.2, 23.7, 14.4.

20: Yield 44%. **^{1}H NMR** (300 MHz, CD_3OD) δ (ppm) 7.10–7.09 (m, 4H), 5.46 (d, J = 3.6 Hz, 1H), 3.90 (t, J = 9.3 Hz, 1H), 3.77–3.71 (m, 3H), 3.59 (dd, J_1 = 9.6 Hz, J_2 = 3.6 Hz, 1H), 3.47 (t, J = 9.2 Hz, 1H), 2.57 (t, J = 7.7 Hz, 2H), 1.62–1.58 (m, 2H), 1.33–1.32 (m, 10H), 0.92 (t, J = 6.8 Hz, 3H). **^{13}C NMR** (75 MHz, CD_3OD) δ (ppm) 156.7, 138.0, 130.2, 118.2, 99.6, 74.9, 74.2, 73.3, 71.5, 62.3, 36.1, 33.0, 32.9, 30.6, 30.4, 30.3, 23.7, 14.4.

4.1.30. 4-n-Octylphenyl β-D-glucopyranoside-6-sulfate (8p)

This substance was prepared from 4-*n*-octylphenyl β-D-glucopyranoside **(19)** using the same procedure as that for **5b.** Yield 42%. **^{1}H NMR** (300 MHz, D_2O) δ (ppm) 6.97–6.90 (m, 4H), 4.72 (d, J = 6.3 Hz, 1H), 4.30–4.27 (m, 1H), 4.17–4.13 (m, 1H), 3.61–3.43 (m, 4H), 2.37 (t, J = 7.1 Hz, 2H), 1.44–1.43 (m, 2H), 1.24–1.23 (m, 10H), 0.88 (t, J = 6.2 Hz, 3H). **^{13}C NMR** (75 MHz, D_2O) δ (ppm) 155.2, 137.3, 129.3, 117.3, 101.7, 75.2, 73.8, 72.8, 68.7, 66.3, 35.0, 31.9, 31.5, 29.5, 29.4, 22.6, 13.9. **HRMS** (ESI) m/z calcd. for $C_{20}H_{32}O_9S$ $[M-H]^-$ 447.1689, found 447.1693.

4.1.31. 4-n-Octylphenyl α-D-glucopyranoside-6-sulfate (*9a*)

This substance was prepared from 4-*n*-octylphenyl α-D-glucopyranoside (**20**) using the same procedure as that for **5b.** Yield 68%. **^{1}H NMR** (300 MHz, D_2O) δ (ppm) 6.96–6.83 (m, 4H), 5.38 (d, J = 3.6 Hz, 1H), 4.28–4.19 (m, 1H), 3.96–3.90 (m, 2H), 3.76–3.59 (m, 3H), 2.3 (t, J = 7.7 Hz, 2H), 1.43–1.42 (m, 2H), 1.24–1.23 (m, 10H), 0.87 (t, J = 6.6 Hz, 3H). **^{13}C NMR** (75 MHz, D_2O) δ (ppm) 154.8, 136.7, 129.1, 117.0, 97.8, 72.8, 71.2, 70.5, 68.7, 66.2, 35.0, 31.9, 31.6, 29.6, 29.5, 22.7, 13.9. **HRMS** (ESI) m/z calcd. for $C_{20}H_{32}O_9S$ $[M-H]^-$ 447.1689, found 447.1695.

4.2. T6PP inhibition measurement using high throughput screening

In order to determine the level of inhibition of T6PP, initial velocities of hydrolysis of T6P in its presence (V_I) and in its absence (V) of 1 mM inhibitor were measured and translated into inhibition activities expressed as the V_I/V ratio. T6PP proteins were prepared by using methods reported previously [19,28]. For the initial velocities determinations (V), 50 μL of a solution in each well of a 96-well plate was prepared to contain T6P (for Mt-T6PP: 400 μM; Bm-T6PP: 200 μM; Sb-T6PP: 690 μM; St-T6PP: 310 μM and As-T6PP: 230 μM), buffer (for Mt-T6PP: 25 mM Hepes pH 7.5, 50 mM NaCl, 5 mM $MgCl_2$, and 5% glycerol; for Sb-T6PP and St-T6PP: 50 mM Hepes pH 7.5, 25 mM NaCl, 2 mM $MgCl_2$, and 5% glycerol; for As-T6PP: 50 mM Tris pH 7.5, 50 mM NaCl, 5 mM $MgCl_2$, 1 mM DTT and 5% glycerol; for Bm-T6PP: 25 mM Tris pH 7.5, 25 mM NaCl, 2 mM $MgCl_2$, 1 mM DTT) and 5–25 nM of freshly purified T6PP, the plate was incubated at room temperature for 5 min and a 5 μL aliquot of the mixture was removed from each and added to a well of another 96 well plate containing 45 μL of the corresponding buffer to generate a 50 μL solution. To each well of the new plate was added 100 μL BioMol Green (Enzo Life Sciences) and the plate was incubated for 30 min. The absorbance of each well at 625 nm was measured using a SpectraMax i3 Multi-Mode Microplate Detection Platform. For determining initial velocities in the presence of inhibitor (V_I), solutions containing T6P, buffer, T6PP, all at the same concentrations as above, and 1 mM inhibitor were incubated in the wells of a 96-well plate and analyzed in the same manner as described above. The initial velocity data (triplicate in all cases) were used to calculate the V_I/V values displayed in Table 2.

4.3. Enzyme inhibition studies

Initial velocities (V_0) for T6PP catalyzed hydrolysis of T6P in presence of different concentrations of inhibitor (0, K_i and 2xK_i) were determined at 25 °C using an EnzCheck Phosphate Assay Kit (Invitrogen). The assay solutions contained 1 mM $MgCl_2$, 0.1 mM sodium azide, 1.0 unit/mL purine nucleoside phosphorylase, and 0.2 mM MESG in 50 mM Tris-HCl (pH 7.5). Absorbance changes were monitored at 360 nm ($\Delta\varepsilon = 9.8\ mM^{-1}cm^{-1}$). The steady-state kinetic constants for T6PP competitive inhibition constants, K_i, were determined for inhibitors by fitting initial velocity data, measured as a function of T6P (0.5 K_m to 5K_m) and inhibitor (0, K_i, 2K_i) concentration, to the following equation:

$$V_0 = V_{max}[S]/\{K_m(1 + [I]/K_i) + [S]\}$$

where V_0 is the initial velocity, V_{max} the maximum velocity, [S] the substrate concentration and K_m the Michaelis-Menten constant calculated for trehalose 6-phosphate, [I] is the inhibitor concentration and K_i the inhibition constant, calculated using SigmaPlot Enzyme Kinetics Module.

Acknowledgements

This study is supported by NIH grant R21 AI103484. We are grateful to Dr. Jeremiah Farelli for gifting the sample of Bm-T6PP used in this work.

Appendix A. Supplementary data

Supplementary data related to this article can be found at http://dx.doi.org/10.1016/j.ejmech.2017.02.001.

References

[1] C. Gancedo, C.L. Flores, The importance of a functional trehalose biosynthetic pathway for the life of yeasts and fungi, FEMS Yeast Res. 4 (2004) 351–359.
[2] N. Benaroudj, D.H. Lee, A.L. Goldberg, Trehalose accumulation during cellular stress protects cells and cellular proteins from damage by oxygen radicals, J. Biol. Chem. 276 (2001) 24261–24267.
[3] T. Hottiger, T. Boller, A. Wiemken, Rapid changes of heat and desiccation tolerance correlated with changes of trehalose content in *Saccharomyces cerevisiae* cells subjected to temperature shifts, FEBS Lett. 220 (1987) 113–115.
[4] J.H. Crowe, L.M. Crowe, D. Chapman, Preservation of membranes in anhydrobiotic organisms: the role of trehalose, Science 223 (1984) 701–703.
[5] J.H. Crowe, F.A. Hoekstra, L.M. Crowe, Anhydrobiosis, Annu. Rev. Physiol. 54 (1992) 579–599.
[6] T. Hottiger, C. Devirgilio, M.N. Hall, T. Boller, A. Wiemken, The role of trehalose synthesis for the acquisition of thermotolerance in yeast. II. Physiological concentrations of trehalose increase the thermal stability of proteins in vitro, Eur. J. Biochem. 219 (1994) 187–193.
[7] N. Avonce, A. Mendoza-Vargas, E. Morett, G. Iturriaga, Insights on the evolution of trehalose biosynthesis, BMC Evol. Biol. 6 (2006) 109.
[8] C.A. Behm, The role of trehalose in the physiology of nematodes, Int. J. Parasitol. 27 (1997) 215–229.
[9] H.N. Murphy, G.R. Stewart, V.V. Mischenko, A.S. Apt, R. Harris, M.S. McAlister, P.C. Driscoll, D.B. Young, B.D. Robertson, The OtsAB pathway is essential for trehalose biosynthesis in *Mycobacterium tuberculosis*, J. Biol. Chem. 280 (2005) 14524–14529.
[10] E.W. Petzold, U. Himmelreich, E. Mylonakis, T. Rude, D. Toffaletti, G.M. Cox, J.L. Miller, J.R. Perfect, Characterization and regulation of the trehalose synthesis pathway and its importance in the pathogenicity of *Cryptococcus neoformans*, Infect. Immun. 74 (2006) 5877–5887.
[11] P. Ngamskulrungroj, U. Himmelreich, J.A. Breger, C. Wilson, M. Chayakulkeeree, M.B. Krockenberger, R. Malik, H.M. Daniel, D. Toffaletti, J.T. Djordjevic, E. Mylonakis, W. Meyer, J.R. Perfect, The trehalose synthesis pathway is an integral part of the virulence composite for *Cryptococcus gattii*, Infect. Immun. 77 (2009) 4584–4596.
[12] S. Puttikamonkul, S.D. Willger, N. Grahl, J.R. Perfect, N. Movahed, B. Bothner, S. Park, P. Paderu, D.S. Perlin, R.A. Cramer Jr., Trehalose 6-phosphate phosphatase is required for cell wall integrity and fungal virulence but not trehalose biosynthesis in the human fungal pathogen *Aspergillus fumigatus*, Mol. Microbiol. 77 (2010) 891–911.
[13] N. Al-Bader, G. Vanier, H. Liu, F.N. Gravelat, M. Urb, C.M. Hoareau, P. Campoli, J. Chabot, S.G. Filler, D.C. Sheppard, Role of trehalose biosynthesis in *Aspergillus fumigatus* development, stress response, and virulence, Infect. Immun. 78 (2010) 3007–3018.
[14] O. Zaragoza, C. Virgilio, J. Pontón, C. Gancedo, Disruption in *Candida albicans* of the TPS2 gene encoding trehalose-6-phosphate phosphatase affects cell integrity and decreases infectivity, Microbiol. 148 (2002) 1281–1290.
[15] J.D. Kormish, J.D. McGhee, The *C. elegans* lethal gut-obstructed gob-1 gene is trehalose-6-phosphate phosphatase, Dev. Biol. 287 (2005) 35–47.
[16] S. Kushwaha, P.K. Singh, M. Shahab, M. Pathak, S.M. Bhattacharya, In vitro silencing of *Brugia malayi* trehalose-6-phosphate phosphatase impairs embryogenesis and in vivo development of infective larvae in jirds, PLoS Negl. Trop. Dis. 6 (2012) e1770.
[17] K.N. Rao, D. Kumaran, J. Seetharaman, J.B. Bonanno, S.K. Burley, S. Swaminathan, Crystal structure of trehalose-6-phosphate phosphatase-related protein: biochemical and biological implications, Protein Sci. 15 (2006) 1735–1744.
[18] A.M. Burroughs, K.N. Allen, D. Dunaway-Mariano, L. Aravind, Evolutionary genomics of the HAD superfamily: understanding the structural adaptations and catalytic diversity in a superfamily of phosphoesterases and allied enzymes, J. Mol. Biol. 361 (2006) 1003–1034.
[19] J.D. Farelli, B.D. Galvin, Z. Li, C. Liu, M. Aono, M. Garland, O.E. Hallett, T.B. Causey, A. Ali-Reynolds, D.J. Saltzberg, C.K. Carlow, D. Dunaway-Mariano, K.N. Allen, Structure of the trehalose-6-phosphate phosphatase from *Brugia malayi* reveals key design principles for anthelmintic drugs, PLoS Pathog. 10 (2014) e1004245.
[20] Y. Miao, J.L. Tenor, D.L. Toffaletti, E.J. Washington, J. Liu, W.R. Shadrick, M.A. Schumacher, R.E. Lee, J.R. Perfect, R.G. Brennan, Structures of trehalose-6-phosphate phosphatase from pathogenic fungi reveal the mechanisms of substrate recognition and catalysis, Proc.Natl. Acad. Sci. U. S. A. 113 (2016) 7148–7153.
[21] S. Shan, H. Min, T. Liu, D. Jiang, Z. Rao, Structural insight into dephosphorylation by trehalose 6-phosphate phosphatase (OtsB2) from *Mycobacterium tuberculosis*, FASEB J. 30 (2016) 3989–3996.
[22] W. Isaac, S.P. Smita, A.J. Kenneth, An induced-fit kinetic mechanism for DNA replication fidelity: direct measurement by single-turnover kinetics, Biochemistry 30 (1991) 526–537.
[23] T.K. Dam, R. Roy, S.K. Das, S. Oscarson, C.F. Brewer, Binding of multivalent carbohydrates to concanavalin A and Dioclea grandiflora lectin. Thermodynamic analysis of the "multivalency effect, J. Biol. Chem. 275 (2000) 14223–14230.
[24] S. Klutts, I. Pastuszak, V. Koroth-Edavana, P. Thampi, Y.T. Pan, E.C. Abraham, J.D. Carroll, A.D. Elbein, Purification, cloning, expression, and properties of mycobacterial trehalose-phosphate phosphatase, J. Biol. Chem. 278 (2003) 2093–2100.
[25] V.K. Edavana, I. Pastuszak, J.D. Carroll, P. Thampi, E.C. Abraham, A.D. Elbein, Cloning and expression of the trehalose-phosphate phosphatase of *Mycobacterium tuberculosis*: comparison to the enzyme from *Mycobacterium smegmatis*, Arch. Biochem. Biophys. 426 (2004) 250–257.
[26] Z. Silva, S. Alarico, M.S. da Costa, Trehalose biosynthesis in *Thermus thermophilus* RQ-1: biochemical properties of the trehalose-6-phosphate synthase and trehalose-6-phosphate phosphatase, Extremophiles 9 (2005) 29–36.
[27] K. Susheela, S.K. Prashant, R.K. Ajay, M.B. Shailja, Cloning, expression, purification and kinetics of trehalose-6-phosphate phosphatase of filarial parasite *Brugia malayi*, Acta Trop. 119 (2011) 151–159.
[28] C. Liu, D. Dunaway-Mariano, P.S. Mariano, Rational design of first generation inhibitors for trehalose 6-phosphate phosphatases, Tetrahedron (2017), http://dx.doi.org/10.1016/j.tet.2017.01.041.
[29] S. Li, Y. Xu, Q. Shen, X. Liu, J. Lu, Y. Chen, T. Lu, C. Luo, X. Luo, M. Zheng, H. Jiang, Non-covalent interactions with aromatic rings: current understanding and implications for rational drug design, Curr. Pharm. Des. 19 (2013) 6522–6533.
[30] D. Chandler, Interfaces and the driving force of hydrophobic assembly, Nature 437 (2005) 640–647.
[31] A. Roberts, S.Y. Lee, E. McCullagh, R.E. Silversmith, D.E. Wemmer, YbiV from *Escherichia coli* K12 is a HAD phosphatase, Proteins 58 (2005) 790–801.
[32] Z. Lu, L. Wang, D. Dunaway-Mariano, K.N. Allen, Structure-function analysis of 2-keto-3-deoxy-D-glycero-D-galactonononate-9-phosphate phosphatase defines specificity elements in type C0 haloalkanoate dehalogenase family members, J. Biol. Chem. 284 (2009) 1224–1233.
[33] The Enzyme FunctionInitiative (EFI), Accessed 29 December 2016, http://kiemlicz.med.virginia.edu/efi/space_tree/view/501036.
[34] N. Bridiau, M. Benmansour, M.D. Legoy, T. Maugard, One-pot stereoselective synthesis of β-*N*-aryl-glycosides by *N*-glycosylation of aromatic amines: application to the synthesis of tumor-associated carbohydrate antigen building blocks, Tetrahedron 63 (2007) 4178–4183.
[35] L. Somsak, N. Felföldi, B. Kónya, C. Hüse, K. Telepo, É. Bokor, K. Czifrák, Assessment of synthetic methods for the preparation of *N*-β-D-glucopyranosyl-*N'*-substituted ureas, -thioureas and related compounds, Carbohydr. Res. 343 (2008) 2083–2093.
[36] É. Bokor, T. Docsa, P. Gergely, L. Somsák, Synthesis of 1-(D-glucopyranosyl)-1,2,3-triazoles and their evaluation as glycogen phosphorylase inhibitors, Bioorg. Med. Chem. 18 (2010) 1171–1180.
[37] J.Y. Winum, A. Casini, F. Mincione, M. Starnotti, J.L. Montero, A. Scozzafava, C.T. Supuran, Carbonic anhydrase inhibitors: *N*-(p-sulfamoylphenyl)-α-D-glycopyrano-sylamines as topically acting antiglaucoma agents in hypertensive rabbits, Bioorg. Med. Chem. Lett. 14 (2004) 225–229.
[38] K.B. Guiseley, P.M. Ruoff, Monosaccharide Sulfates. I. Glucose 6-sulfate. preparations, characterization of the crystalline potassium salt, and kinetic studies, J. Org. Chem. 26 (1961) 1248–1254.
[39] I. Laville, S. Pigaglio, J.C. Blais, B. Loock, P. Maillard, D.S. Grierson, J. Blais, A study of the stability of tri(glucosyloxyphenyl)chlorin, a sensitizer for photodynamic therapy, in human colon tumoural cells: a liquid chromatography and MALDI-TOF mass spectrometry analysis, Bioorg. Med. Chem. 12 (2004) 3673–3682.
[40] C. Liu, P.S. Mariano, An improved method for the large scale preparation of α,α′-trehalose-6-phosphate, Tetrahedron Lett. 56 (2015) 3008–3010.
[41] Y. Zhou, J. Lia, Y. Zhan, Z. Pei, H. Dong, Halide promoted organotin-mediated carbohydrate benzylation: mechanism and application, Tetrahedron 69 (2013) 2693–2700.
[42] B.B. Liau, B.C. Milgram, M.D. Shair, Total syntheses of HMP-Y1, hibarimicinone, and HMP-P1, J. Am. Chem. Soc. 134 (2012) 16765–16772.
[43] S. Tani, S. Sawadi, M. Kojima, S. Akai, K. Sato, A novel method for regioselective ring-opening reduction of 4,6-*O*-benzylidene hexopyranoside derivatives using $CoCl_2$ and $BH_3 \cdot THF$, Tetrahedron Lett. 48 (2007) 3103–3104.
[44] O.M.T. Pearce, A. Varki, Chemo-enzymatic synthesis of the carbohydrate antigen N-glycolylneuraminic acid from glucose, Carbohydr. Res. 345 (2010) 1225–1229.
[45] X. Dai, S. Wu, W. Yang, Chemical Synthesis Process for Preparing Gastrodin and its Analogous Henolic Glycoside Formula (I), 2003. Zhuanli Shenqing Gongkai Shuomingshu CN1428345 A.
[46] L. Kröger, J. Thiem, Synthesis and evaluation of glycosyl donors with novel leaving groups for transglycosylations employing β-galactosidase from bovine testes, Carbohydr. Res. 342 (2007) 467–481.
[47] D.E. Green, C.L. Ferreira, R.V. Stick, B.O. Patrick, M.J. Adam, C. Orvig,

Carbohydrate-bearing 3-hydroxy-4-pyridinonato complexes of gallium(III) and indium(III), Bioconjugate Chem. 16 (2005) 1597–1609.
[48] K. Sasaki, Y. Nishida, M. Kambara, H. Uzawa, T. Takahashi, T. Suzuki, Y. Suzuki, K. Kobayashi, Design of *N*-acetyl-6-sulfo-β-D-glucosaminide-based inhibitors of influenza virus sialidase, Bioorg. Med. Chem. 12 (2004) 1367–1375.
[49] D. Loganathan, G.K. Trivedi, Phase-transfer-catalyzed D-glucosylation: synthesis of benzoylated aryl β-D-glucopyranosides and β-D-glucopyranosyl-substituted cinnamates, Carbohydr. Res. 162 (1987) 117–125.
[50] H. Wen, C. Lin, L. Que, H. Ge, L. Ma, R. Cao, Y. Wan, W. Peng, Z. Wang, H. Song, Synthesis and biological evaluation of helicid analogues as novel acetylcholinesterase inhibitors, Eur. J. Med. Chem. 43 (2007) 166–173.
[51] R.R. France, R.G. Compton, B.G. Davis, A.J. Fairbanks, N.V. Rees, J.D. Wadhawan, Selective electrochemical glycosylation by reactivity tuning, Org. Biomol. Chem. 2 (2004) 2195–2202.